High-affinity Anticalins with aggregation-blocking activity directed against the Alzheimer β-amyloid peptide

Sabine Rauth*[1], Dominik Hinz*[1], Michael Börger*, Markus Uhrig†, Manuel Mayhaus†, Matthias Riemenschneider† and Arne Skerra*[2]

*Munich Center for Integrated Protein Science (CIPS-M) and Lehrstuhl für Biologische Chemie, Technische Universität München, 85354 Freising (Weihenstephan), Germany
†Department of Psychiatry and Psychotherapy, Universitätsklinikum des Saarlandes, 66421 Homburg/Saar, Germany

Amyloid beta (Aβ) peptides, in particular Aβ42 and Aβ40, exert neurotoxic effects and their overproduction leads to amyloid deposits in the brain, thus constituting an important biomolecular target for treatments of Alzheimer's disease (AD). We describe the engineering of cognate Anticalins as a novel type of neutralizing protein reagent based on the human lipocalin scaffold. Phage display selection from a genetic random library comprising variants of the human lipocalin 2 (Lcn2) with mutations targeted at 20 exposed amino acid positions in the four loops that form the natural binding site was performed using both recombinant and synthetic target peptides and resulted in three different Anticalins. Biochemical characterization of the purified proteins produced by periplasmic secretion in *Escherichia coli* revealed high folding stability in a monomeric state, with T_m values ranging from 53.4 °C to 74.5 °C, as well as high affinities for Aβ40, between 95 pM and 563 pM, as measured by real-time surface plasmon resonance analysis. The central linear VFFAED epitope within the Aβ sequence was mapped using a synthetic peptide array on membranes and was shared by all three Anticalins, despite up to 13 mutual amino acid differences in their binding sites. All Anticalins had the ability – with varying extent – to inhibit Aβ aggregation *in vitro* according to the thioflavin-T fluorescence assay and, furthermore, they abolished Aβ42-mediated toxicity in neuronal cell culture. Thus, these Anticalins provide not only useful protein reagents to study the molecular pathology of AD but they also show potential as alternative drug candidates compared with antibodies.

Key words: Aβ peptide, lipocalin, neurodegeneration, protein engineering.

INTRODUCTION

Alzheimer's disease (AD) is the most prevalent form of dementia, with 10 % of the human population older than 65 years and 40 % older than 85 years affected [1]. Apart from certain forms of inherited AD [2], age is the major risk factor associated with this devastating neurodegenerative disease, thus currently causing a dramatic increase in AD incidence due to the steadily aging Western communities.

Histologically, AD is characterized by two hallmarks: (i) the deposition of aggregated amyloid beta (Aβ) peptides in extracellular plaques and (ii) the formation of intracellular neurofibrillary tangles comprising the hyperphosphorylated protein tau. Aβ peptides are generated *in vivo* by proteolytic processing of the amyloid-β precursor protein (APP) [3], a large integral membrane protein expressed at high levels in the brain [4]. Sequential proteolysis by β-secretase and the γ-secretase complex yields lipophilic Aβ peptides with predominantly 40 and also 42 amino acids (Aβ40 and Aβ42 respectively, comprising residues 672–711/713; UniProt ID P05067), of which the latter shows even stronger aggregation propensity [5].

The amyloid hypothesis places Aβ and its pronounced aggregation behaviour at the top of a cascade which eventually leads to extensive cell death and neuronal damage [6]. An imbalance between production and clearance of Aβ peptides and a shift in the ratio between Aβ40 and Aβ42 leads to the accumulation of Aβ peptide species which have a tendency to spontaneously self-associate. This results in the formation of soluble oligomers as well as protofibrils and, eventually, insoluble fibrils with predominant β-pleated sheet secondary structure [3]. However, more recent findings suggest that it is less the insoluble amyloid plaque protein/peptide but rather the soluble dimeric or early oligomeric assemblies of Aβ that constitute the major toxic species involved in AD pathogenesis [7–9].

Consequently, rational attempts towards AD therapy currently aim at prevention of the accumulation of such toxic oligomeric Aβ forms in several ways: (i) by slowing down Aβ biogenesis, (ii) by inhibiting Aβ oligomerization or (iii) by promoting Aβ clearance [10]. Decreasing the cellular production of pathogenic Aβ peptides seems to be the most direct approach in this scenario. Yet, inhibition (or stimulation) of proteases involved in APP processing (i.e. β-, γ- and α-secretases) bears a risk of severe side effects as shown e.g. by the failure of the γ-secretase inhibitor semagacestat in a phase III clinical trial [11].

In contrast, Aβ immunotherapy has gained increasing attention as a potential strategy to specifically suppress neurotoxicity [10]. Up to now, more than ten humanized or fully human antibodies directed against Aβ have reached advanced clinical trial stages [12,13]. Both active immunization, i.e. vaccination with Aβ peptides or their derivatives, and passive immunization

Abbreviations: Aβ, amyloid beta; AD, Alzheimer's disease; APP, amyloid-β precursor protein; BBB, blood–brain barrier; BIO, biotin; DIG, digoxigenin; HFIP, 1,1,1,3,3,3-hexafluoro-2-propanol; IMAC, immobilized metal ion affinity chromatography; Lcn2, human lipocalin 2; NGAL, neutrophil gelatinase-associated lipocalin; SEC, size exclusion chromatography; SPR, surface plasmon resonance; TEM, transmission electron microscopy; TEV, tobacco etch virus; ThT, Thioflavin T; TrxA, thioredoxin.

[1] These authors contributed equally to this work.

[2] To whom correspondence should be addressed (email skerra@tum.de).

via administration of monoclonal anti-Aβ antibodies have demonstrated positive effects *in vivo* with regard to amyloid burden, plaque deposits, neuritic dystrophy as well as behavioural and memory deficits both in animal models and in AD patients [14,15].

Nevertheless, the first clinical trials on active immunization of AD patients were aborted due to the occurrence of meningoencephalitis [16]. Indeed, in this setting inflammatory autoimmune reactions may be triggered in various ways such as by activation of Aβ-reactive T-lymphocytes in the periphery and their migration to Aβ-plaques within the brain [17] or, more generally, via Fc-mediated activation of microglial cells by plaque-bound antibodies as well as phagocytosis.

Conversely, according to the so-called peripheral sink hypothesis [18], systemically administered anti-Aβ antibodies may sequester Aβ peptides in the blood plasma and, thus, promote a net efflux of Aβ from the brain by shifting the (bio)chemical equilibrium, which could lead to decreased plaque burden in the brain. Most notably, this alternative mechanism of Aβ clearance is independent of Fc-mediated immune effector functions and also circumvents the need for therapeutic agents to cross the blood–brain barrier (BBB).

The therapeutic potential of Fc-independent Aβ clearance mechanisms on the one hand and the risk of full-size antibodies evoking an inflammatory response in the brain on the other, along with the large size and generally poor BBB penetration of antibodies, have inspired alternative approaches to the development of biopharmaceuticals. Indeed, several laboratories have examined antibody fragments such as $F(ab')_2$ and scFv for their potential to treat AD [19–21]. In addition, engineered protein scaffolds have been generated with specificities for different forms of the Aβ peptide; these include nanobodies derived from the V_HH domain of camelids or sharks [22,23], affibodies, artificial binding proteins based on a modified Z domain of the *staphylococcal* protein A [24,25], as well as designed proteins based on the consensus Ankyrin fold, so-called DARPins [26].

In this context, the lipocalins offer a particularly versatile protein scaffold of human origin that appears suitable to tightly bind and scavenge small molecules including peptides such as Aβ [27]. Lipocalins are small, robust proteins, typically comprising 150–180 residues, which serve for the transport or storage of poorly soluble or chemically sensitive biochemical compounds, in particular vitamins, hormones and secondary metabolites, in many organisms [28]. Several members of this protein family are found in human plasma [29].

The lipocalin fold comprises a circularly closed antiparallel sheet of eight β-strands against which an α-helix is packed from one side. At its open end the β-barrel supports four loops with variable lengths, sequences and conformations, which form the entrance to the natural ligand pocket. This loop region, which structurally resembles the hypervariable loops of antibodies [30], has been successfully exploited to generate tailored binding proteins via selection from combinatorial random libraries [31]. This has enabled the combinatorial engineering of so-called Anticalins having tight binding properties and specificities for various targets, ranging from small molecules to large protein ligands [27].

One of the human lipocalin scaffolds that has been employed with particular success for the generation of a series of high affinity Anticalins [32–34] is the human lipocalin 2 (Lcn2), also known as neutrophil gelatinase-associated lipocalin (NGAL) or, more recently, siderocalin [35]. By specifically scavenging Fe^{3+} ions bound to certain bacterial siderophores, natural Lcn2 plays a pivotal role as bacteriostatic agent in the innate immune response. Lcn2 is a 178 amino acid plasma glycoprotein that differs from other typical members of the lipocalin family by its rather wide ligand pocket and its remarkable affinity for the natural ligand Fe^{III}·enterobactin ($K_D = 0.4$ nM).

Here, we report the engineering of Anticalins towards Aβ40 using phage display selection from an Lcn2-based random library utilizing different peptide targets. These Anticalins efficiently block Aβ aggregation *in vitro* and reduce Aβ toxicity in neuronal cell culture.

MATERIALS AND METHODS

Aβ targets

Synthetic Aβ40 and Aβ42 were obtained from the Keck Biotechnology Resource Laboratory (Yale University), the biotinylated peptides Aβ40-BIO (equipped with a C-terminal Nε-biotinyl-lysine) as well as Aβ(1–11)-BIO and Aβ(16–27)-BIO (biotin attached to the C-terminus via an ethylendiamine linker) were from Peptide Specialty Laboratories.

To prepare defined solutions of the monomeric Aβ peptides, synthetic lyophilized Aβ40 and Aβ40-BIO were dissolved in 1,1,1,3,3,3-hexafluoro-2-propanol (HFIP; Sigma–Aldrich) for 12 h at room temperature without agitation (adapted from [5,36]). After that, the organic solvent was removed with a SpeedVac Univapo UVC 150H (UniEquip). Finally, the solid peptide was resuspended under vortex-mixing in a suitable volume of doubly distilled cold H_2O, sonicated for 15 min at 4 °C, and sterile-filtrated with a Costar Spin-X centrifuge tube filter, 0.45 μm pore cellulose acetate membrane (Corning Life Sciences). The solubilized monomeric Aβ40 or Aβ40-BIO was immediately used for experiments.

For cell culture assays and transmission electron microscopy (TEM), the synthetic lyophylized Aβ42 was dissolved in 50 % (v/v) acetonitrile (Merck) and aliquoted at approximately 100 μg. The solvent was evaporated under a gentle stream of nitrogen and the solid residue was stored at −20 °C. Prior to use, an aliquot was redissolved in 1 volume (50 μl) of 5 mM NaOH and subsequently combined by vortex-mixing with 1 volume of 20 mM Tris/HCl, pH 6.8 (modified from [37]). Concentrations were measured by BCA protein assay (Pierce / Thermo Fisher Scientific) and adjusted to 200 μM using PBS. This solution of 200 μM Aβ42 was 'aged' by incubation for 6 h at 4 °C [38] without agitation and then diluted to a final concentration of 10 μM in RPMI-1640 medium without L-glutamine and Phenol Red (Sigma).

The more soluble shorter peptides were directly dissolved in the buffer of choice.

Aβ fusion proteins

The gene for a His_6-tagged fusion between *Escherichia coli* maltose-binding protein (MBP) and Aβ40 (MBP-Aβ40) [39] was constructed in a step-wise manner and cloned on the expression vector pASK75 [40]. To this end, the sequence of MBP was amplified via PCR from a cloned DNA template and the sequence of Aβ40 including an N-terminal His_6-tag as well as the cleavage site of the tobacco etch virus (TEV) protease was generated via gene synthesis using PCR assembly with four overlapping oligodeoxynucleotides [41]. After induction of recombinant gene expression in the cytoplasm of *E. coli* strain JM83 [42] for 3 h at 37 °C using anhydrotetracycline (Acros Organics) the bacterial cells were disrupted using a French pressure cell (SLM Aminco) and insoluble material was removed via centrifugation. The fusion protein was purified from the soluble supernatant via immobilized metal ion affinity chromatography (IMAC) on

an IDA-Sepharose fast flow column (GE Healthcare) in 20 mM Tris/HCl, 150 mM NaCl, pH 8.0 and eluted with a concentration gradient of up to 200 mM imidazole/HCl. Fractions containing the recombinant protein were supplemented with 5 mM EDTA and subsequently dialysed against PBS for purification via size exclusion chromatography (SEC) on Superdex 200 (GE Healthcare).

The coding region for the Trx-Aβ28 hybrid protein was obtained by insertion of a PCR-amplified DNA fragment encoding residues 1–28 of Aβ into the cloned gene for *E. coli* thioredoxin (TrxA), carrying a His_6-tag, to replace the active site loop of this protein scaffold [43], again employing pASK75. After gene expression as above, Trx-Aβ28 was purified via IMAC and SEC, this time on a Superdex 75 column (GE Healthcare).

MBP and TrxA without the Aβ moieties, which were expressed and purified in the same manner, served as control proteins. Protein purity was assessed by SDS/PAGE and staining with Coomassie Brilliant Blue R-250 [44]. Protein concentration was quantified via absorption at 280 nm using molar absorption coefficients calculated with the ExPASy ProtParam Tool [45].

Library generation and phage display selection of Aβ-specific Lcn2 variants

A combinatorial library of approximately 1×10^{10} independent Lcn2 variants had been generated on the basis of the cloned cDNA [46] in a one-pot assembly reaction employing 10 overlapping oligodeoxynucleotides carrying degenerate NNK codons at the mutated positions [47]. Phage display and phagemid panning were essentially performed according to published procedures [31].

Two phage display selections were performed in parallel for the target Aβ40-BIO, each comprising 4 cycles, differing only in the elution methods applied during cycles 1 and 2. To this end, each about 10^{12} phagemids dissolved in PBS (4 mM KH_2PO_4, 16 mM Na_2HPO_4, 115 mM NaCl, pH 7.4) were blocked with 2 % (w/v) BSA in PBS/T (PBS containing 0.1 % (v/v) Tween 20) for 1 h at room temperature. For each panning step, two aliquots of streptavidin-coated magnetic beads (Dynabeads M-280 Streptavidin; Dynal/Invitrogen; or Streptavidin Magnetic Particles; Roche Diagnostics) were prepared by washing with PBS/T and blocking with PBS/T containing 2 % (w/v) BSA for 1 h. For depletion of non-specific binders the phagemids from above were first incubated with one aliquot (250 μg) of the magnetic particles for 30 min, followed by bead collection on a magnetic stand (Promega) for 2 min. The supernatant containing the unbound phagemid fraction was transferred to a new tube and incubated under gentle rotation for 1–2 h with 100 nM Aβ40-BIO in a total volume of 400 μl PBS/T with 2 % (w/v) BSA. For pull-down of phagemid·target complexes, this mix was then incubated for 30 min with the second aliquot (500 μg) of magnetic beads. After magnetic collection, the supernatant was discarded and the beads with bound phagemids were washed 10 times with 400 μl PBS/T. In cycles 1 and 2, bound phagemids from the two setups were both eluted under denaturing conditions, either with an acidic buffer or in the presence of urea. To this end, beads were incubated under gentle rotation (i) for 10 min with 350 μl 0.1 M glycine/HCl pH 2.2, followed by immediate neutralization with 55 μl 0.5 M Tris base, or (ii) for 30 min with 400 μl 4 M urea in PBS, followed by dilution with 1 ml PBS. In cycles 3 and 4, the concept of competitive elution was applied by mixing the beads with 400 μl of a 100 μM solution of non-biotinylated Aβ40 and incubating under gentle rotation for 1 h. After these elution steps, the stripped beads were each time incubated with a 1 ml culture of exponentially growing XL1-Blue cells [48] to recover undissociated phagemids by way of bacterial infection. These cultures were finally pooled with XL1-Blue cells that had been infected with the eluted phagemid solutions and were then used for phagemid amplification according to a published procedure [31].

Phage display selection against the digoxigenin (DIG)-labelled Trx-Aβ28 hybrid protein was conducted as described above with a few modifications. In this case, a suspension of magnetic beads coated with an anti-DIG antibody (Europa Bioproducts) was blocked with 2 % (w/v) BSA in PBS/T (cycles 1–2) or 2 % (w/v) skim milk (Sucofin; TSI) in PBS/T (cycles 3–6). To prevent enrichment of TrxA-specific variants, phagemids were first blocked with the above blocking solutions, depleted once by incubation with blocked anti-DIG beads and then incubated for 30 min with ∼400 μl of a 15 μM solution of recombinant TrxA under gentle rotation. After that, 3 μl of a 13.5 μM solution of DIG-labelled Trx-Aβ28 – in which free thiol groups had been masked, after DIG-labelling, by incubation with a 50-fold excess of iodoacetamide for 1 h, followed by SEC purification – was added at a final concentration of 100 nM and the mix (400 μl) was incubated under gentle rotation for 1–2 h to allow phagemid·target complex formation. Subsequently, the blocked beads were added, followed by incubation for 30 min under gentle rotation. Then, the beads were collected as above and washed 10 times with 500 μl PBS/T. Finally, bound phagemids were eluted in 400 μl PBS containing 4 M urea for 30 min under gentle rotation, followed by dilution with 1 ml PBS. Again, the stripped beads were also incubated with 1 ml exponentially growing XL1-Blue cells to recover remaining tightly bound phagemids prior to phagemid amplification.

Screening for Aβ-specific Lcn2 variants via ELISA and filter-sandwich colony assay

After subcloning of the mutated central Lcn2 gene cassette from enriched gene pools after phage display selection on a vector for soluble protein production in the periplasm of *E. coli*, Aβ-specific variants were identified in 'direct' or 'capture' screening ELISAs [31]. In the 'direct' ELISA, Aβ40, Trx-Aβ28, or the negative control proteins ovalbumin and TrxA, were coated on a 96-well MaxiSorp polystyrene microtiter plate (Nunc) at a concentration of 0.5 μM. In the 'capture' setup, soluble Lcn2 variants in crude small-scale periplasmic extracts carrying the C-terminal *Strep*-tag II [49] were selectively captured on a 96-well MaxiSorp polystyrene microtiter plate coated with 50 μl of 10 μg/ml *Strep*MAB-Immo (IBA) and, subsequently, 0.5 μM biotinylated Aβ40 or biotinylated ovalbumin were applied.

Alternatively, screening was performed by means of an *E. coli* filter-sandwich colony assay according to a published protocol [31]. In this assay, Aβ-specific variants – secreted from bacterial colonies and functionally adsorbed on to a filter membrane – were detected by incubation with 100 nM Trx-Aβ28 labelled with DIG groups, followed by an anti-DIG Fab/alkaline phosphatase (AP) conjugate (Roche Diagnostics) and chromogenic reaction.

Expression, purification and biochemical characterization of Anticalins

Aβ-specific Lcn2 variants were prepared via soluble periplasmic secretion in 2 L shake flask cultures [31] using *E. coli* JM83 [42] or *E. coli* TG1/F^- [32]. Larger amounts were produced in an 8 litre fed-batch fermenter using *E. coli* W3110 [50] as previously described [46]. Wild-type Lcn2 was expressed in *E. coli* BL21 [51] as this strain lacks the natural ligand enterobactin [35]. Anticalins

were purified by *Strep*-tag II affinity chromatography [49] and SEC on a Superdex 75 HR 10/30 column using buffers suitable for subsequent assays. Protein purity was checked by SDS/PAGE [44]. Protein concentration was measured via absorption at 280 nm using molar absorption coefficients calculated with the ExPASy ProtParam Tool [45].

Thermal stability of Anticalins was assessed by CD spectroscopy of purified protein samples at a concentration of 25 μM in 20 mM KH_2PO_4, 50 mM K_2SO_4, pH 7.5 using a J810 spectropolarimeter (Jasco). Wavelengths were 209 nm for H1G1, H1GA, H1GV and S1A4 and 210 nm for wtLcn2 and US7. CD measurements and data analysis were performed as previously described [52].

Site-directed mutagenesis of Cys^{36} in H1G1

A single unpaired Cys residue in the selected Lcn2 variant H1G1 was replaced by Ala or Val via PCR mutagenesis using *Taq* DNA polymerase (Fermentas) and the oligodeoxynucleotides 5′-G GAC AAC CAA TTC CAT GGG AAG TGG TAT GTG GTA GGT GYT GCA GGG AAT GTG TTG CTC and 5′-GCT GCC GTC GAT ACA CTG (Thermo Fisher Scientific). In a single PCR reaction the central gene cassette of H1G1 including the two *Bst*XI sites was amplified whereby the degenerate oligonucleotide allowed the substitution of Cys36 (TGT) with Ala (GCT) and Val (GTT) in the amplificate. Subsequently, the PCR product was cut with *Bst*XI and inserted into the analogously cut expression vector.

Measurement of binding activity via ELISA and SPR

For affinity measurements, capture ELISAs were performed with 1 μM of purified Lcn2 variants as described above for the crude periplasmic extracts. Dilution series of biotinylated Aβ targets, or control proteins, were added and binding was detected with an ExtrAvidin/AP conjugate (Sigma–Aldrich), followed by chromogenic reaction.

Kinetic affinity data were measured on Biacore T100 (Anticalins H1GA and US7 with immobilized Aβ40) and Biacore X (immobilized MBP-Aβ40) instruments (Biacore) using PBS supplemented with 0.005 % (v/v) Surfactant P20 or Tween 20 as running buffer. ~350 RU of Aβ40 and ~1300 RU of MBP-Aβ40 were covalently immobilized on CM5 (Biacore) or CMD 200l chips (XanTec Bioanalytics) using amine coupling chemistry. Dilution series of the purified Lcn2 variants were applied at flow rates of 30 μl/min (Biacore T100) or 20 μl/min (Biacore X). The data were double-referenced by subtraction of the corresponding signals measured for the control channel and of the average of three buffer injections [53]. Kinetic parameters were determined using Biacore T100 Evaluation Software V2.0.3 or BiaEvaluation Software V 4.1 [54]. The equilibrium dissociation constants were calculated as $K_D = k_{off}/k_{on}$ and the statistical error was estimated as previously described [33].

Peptide epitope mapping

For mapping of the linear epitope within the Aβ peptide sequence recognized by the selected Lcn2 variants, one set of successive hexamers and one set of successive decamers, each covering the entire sequence of Aβ40 and dislocated by 1 amino acid, were synthesized on an amino-PEG500-derivatized cellulose membrane (Intavis) using the SPOT technique [55]. The fluorenylmethoxycarbonyl solid-phase peptide synthesis was perfomed on a MultiPep RS instrument (Intavis) leading to C-terminally immobilized peptides. After acetylation of the N-termini, side chains were deprotected with trifluoroacetic acid as described [56]. The *Strep*-tag II peptide [49] synthesized on the same membrane served as an internal positive control for detection. The membrane was washed once with ethanol, three times with PBS, blocked with 3 % (w/v) BSA in PBS/T for 1 h and washed three times with PBS/T. Then, the membrane was incubated with the Lcn2 variants H1G1 (100 nM), S1A4 (50 nM), US7 (100 nM) or wtLcn2 (100 nM) in PBS/T for 1 h, followed by washing three times with PBS/T. The membrane was subsequently incubated with a 1:1500 dilution of streptavidin/AP conjugate (GE Healthcare) in PBS/T for 1 h to detect bound Anticalins via the *Strep*-tag II. Finally, the membrane was washed three times with PBS/T and once in AP buffer (100 mM Tris/HCl pH 8.8, 100 mM NaCl, 5 mM $MgCl_2$), prior to signal development via chromogenic reaction with 5-bromo-4-chloro-3-indolyl phosphate, 4-toluidine salt (AppliChem) and Nitro Blue Tetrazolium (AppliChem) in AP buffer according to a standard procedure [56].

Thioflavin T aggregation assay

A freshly prepared solution of monomeric Aβ40 was immediately used for setup of the aggregation assay. Two hundred and fifty microlitres of 2 mg/ml (462 μM) Aβ40 in H_2O was mixed with a 250 μl PBS solution of the Lcn2 variant at different molar ratios or of BSA. Aggregation reactions were performed in triplicates at 37 °C in 2 ml DNA LoBind Tubes (Eppendorf) with stirring at 500 rpm using a 5 mm magnetic bar. For fluorescence measurement, 20 μl samples were periodically removed and mixed with 180 μl of a 55.6 μM Thioflavin T (ThT) (Sigma–Aldrich) solution in PBS/H_2O 1:1 and analysed in a FluoroMax-3 spectrofluorimeter (HORIBA Jobin Yvon) using an excitation wavelength of 450 nm and an emission wavelength of 482 nm. Measured ThT fluorescence intensities were set to zero for $t = 0$ and referenced to the asymptotic value of the fluorescence intensity of aggregating Aβ40 without additives. Normalized fluorescence data *versus* time (t) were fitted using KaleidaGraph (Synergy Software) to a mathematical model for an autocatalytic reaction [57]:

$$f(\mathrm{t}) = f_\infty \frac{\mathrm{e}^{(k_\mathrm{e}+k_\mathrm{n})t} - 1}{(k_\mathrm{e}/k_\mathrm{n}) + \mathrm{e}^{(k_\mathrm{e}+k_\mathrm{n})t}}$$

Therein, k_n is the nucleation rate, k_e the fibril elongation rate and f_∞ the asymptotic end fluorescence. k_n inversely reflects the lag behaviour at the beginning of the aggregation reaction whereas k_e represents the steep slope of the exponential phase for subsequent fibril growth.

Transmission electron microscopy

A 200 μM solution of Aβ42, aged for 6 h at 4 °C in a 1:1 mixture of 5 mM NaOH and 20 mM Tris/HCl, pH 6.8, was diluted to 10 μM in RPMI-1640 medium (Sigma) in the presence or absence of equimolar concentrations of Anticalin or MAb 6E10 (Covance). After incubation for 72 h at 37 °C the mixture was fixed on poly-L-lysine coated copper grids (Plano) and negatively stained with 1 % (w/v) uranyl acetate. Anticalins without Aβ42 were diluted in RPMI-1640 medium and equally treated. TEM images were recorded with a Tecnai Biotwin 120 kV transmission electron microscope (FEI) at 150000-fold magnification.

Neuronal cytotoxicity assay

Cytotoxicity of Aβ42, Anticalins or Aβ42/Anticalin mixtures was assessed via a metabolic assay using 3-(4,5-dimethylthiazol-2-yl)-2,5-diphenyltetrazolium bromide (MTT; Roche).

PC12 cells (A.T.C.C. no. CRL-1721) were seeded on to BioCoat Collagen IV 96-well Microtest Plates (BD Bioscience) and grown in RPMI-1640 medium without L-glutamine and Phenol Red but supplemented with 10 % (v/v) horse serum (Sigma) and 5 % (v/v) FCS (Gibco). After 24 h, 150 ng/ml NGF-β (Sigma) was added to the cells, which were then incubated for 3 days at 37 °C. Differentiation was evaluated by the extent (length and number) of outgrowing neurites via light microscopy using a Trino Plan IT400 inverted trinocular microscope (VWR). At least 60–95 % of all cells showed characteristic signs of differentiation in all experiments. A freshly prepared 200 μM solution of Aβ42 was aged for 6 h at 4 °C as described further above, then diluted with RPMI-1640 medium (without L-glutamine and Phenol Red) and supplemented with concentrated stock solutions of the purified Anticalins to reach final concentrations of 10 μM Aβ42 as well as 0, 2, 5 or 10 μM of each Anticalin. This mixture was then added to the differentiated PC12 cells and incubated for 72 h at 37 °C. Finally, Aβ42-induced cytotoxicity was evaluated by the MTT assay directly in the 96-well cell culture plates according to the manufacturer's recommendations and visually confirmed by light microscopy after staining with Trypan Blue (Sigma). Signals were quantified using an Infinite M 200 NanoQuant microplate reader (Tecan) by measuring the absorption difference between 570 nm and 690 nm (corresponding to the background signal). The same buffer used to dissolve Aβ42 was employed as a negative control whereas 10 % (v/v) ethanol in RPMI-1640 medium served as a positive control to estimate cytotoxic effects. Each treatment was applied in 4–8 wells of the same 96-well plate, which always included controls, and each experiment was performed at least three times, thus allowing calculation of the mean values and the standard errors of the mean (S.E.M.). For comparison, solutions of the Anticalins alone (without Aβ42) were added to the differentiated cells, in the presence of RPMI-1640 medium without L-glutamine and Phenol Red, and were tested in the same assay.

RESULTS

Aβ target preparation and selection of cognate Anticalins

Due to the well-known properties of oligomerization, fibrillation, aggregation, precipitation and adsorption *in vitro* and the associated difficulties in handling especially the Aβ42 peptide in aqueous solution [58,36] we chose the less pathogenic Aβ40, as well as some shorter fragments, as soluble targets for the selection of cognate Anticalins via phage display. Suitable monomeric Aβ peptides were prepared both by chemical synthesis and via genetic engineering in various formats to serve different purposes (Figure 1):

- full length synthetic biotin-labelled Aβ40 for phage display selection and affinity determination;
- synthetic biotin-labelled Aβ fragments Aβ1–11 and Aβ16–27 for locating the epitopes of selected Anticalins;
- full length synthetic Aβ40 for aggregation analysis;
- full length synthetic oligomeric Aβ42 for cell culture assays of neurotoxicity;
- a recombinant fusion protein of Aβ40 with the highly soluble maltose-binding protein (MBP) of *E. coli* for affinity measurements [39];
- a hybrid protein with thioredoxin of *E. coli* (TrxA) carrying an insertion of residues 1–28 of Aβ in the active site loop (Trx-Aβ28) for phage display selection of Anticalins [43] after conjugation with DIG.

A targeted random library derived from human Lcn2 was used for phagemid panning against some of these Aβ targets. This library had an optimized design with 20 specifically randomized positions distributed across the loops and the upper part of the cavity in the lipocalin scaffold based on earlier designs for hapten- and protein-targeting Lcn2 random libraries [32,33]. This kind of library (cf. Figure 1C) was successfully applied already – though using triplet codon mutagenesis in this case – for the generation of Anticalins directed against the fibronectin extra-domain B [34].

After various unsuccessful initial attempts and careful optimization of experimental conditions, two phage display campaigns led to the selection of a set of Aβ-specific Anticalins: one obtained with the biotinylated full-length Aβ40 peptide (Aβ40-BIO) and another one after panning against the DIG-labelled Trx-Aβ28 fusion protein (Trx-Aβ28-DIG). In these experiments, Aβ40-BIO and Trx-Aβ28-DIG were incubated with the Anticalin phagemid library in solution and complexes with the labelled Aβ targets were subsequently captured by appropriately functionalized magnetic beads followed by elution with acid or urea, including some competitive elution steps in case of the selection with Aβ40-BIO (for details see Materials and Methods).

From the resulting pools of enriched phagemids, the coding DNA region for the central part of the Lcn2 variants was subcloned on a vector for soluble expression [31], encoding a fusion protein with the *Strep*-tag II [49]. In case of the Aβ40 target, lipocalin variants were expressed in *E. coli* cultures in microtitre plates and subjected to a screening ELISA against the Aβ40 peptide (Supplementary Figure S1). In case of the Trx-Aβ28 target, a vector encoding a fusion protein between Lcn2 and a bacterial albumin-binding domain (ABD), with the *Strep*-tag II serving as linker, was used in order to conduct an *E. coli* colony filter-sandwich screen [31,59] for binding of Trx-Aβ28-DIG applied in solution (Supplementary Figures S1C and S1D).

Several clones from the phage display selection against the synthetic full length Aβ40 peptide that showed high signals in the screening ELISA – but low or no signals for dummy targets such as ovalbumin – were subjected to DNA sequencing. Interestingly, just two different Lcn2 variants, dubbed H1G1 and S1A4, were found (among 356 clones screened and 13 sequences investigated), thus indicating strong enrichment, irrespective of the method chosen for elution during phagemid panning (see Materials and Methods).

Similarly, in the filter-sandwich colony screen of the clones selected against the recombinant hybrid protein Trx-Aβ28, just one Anticalin candidate with pronounced binding activity, US7, was initially identified. Later on, pools of phagemids from the same panning campaign were also subjected to a screening ELISA with immobilized Trx-Aβ28 and, again, US7 showed up in all of the four most prominent hits. Notably, all three selected Anticalin candidates, H1G1, S1A4 and US7, exhibited mutually distinct amino acid sequences that differed in 13–14 residues, and only a few positions (52, 68, 70, 79, 81, 134) were shared among them (Figure 1C).

Preparative expression, further engineering and stability analysis of selected Anticalins

The Anticalins H1G1, S1A4 and US7 were individually expressed in *E. coli* via periplasmic secretion – to ensure formation of the single disulfide bond – as soluble proteins both in the shake

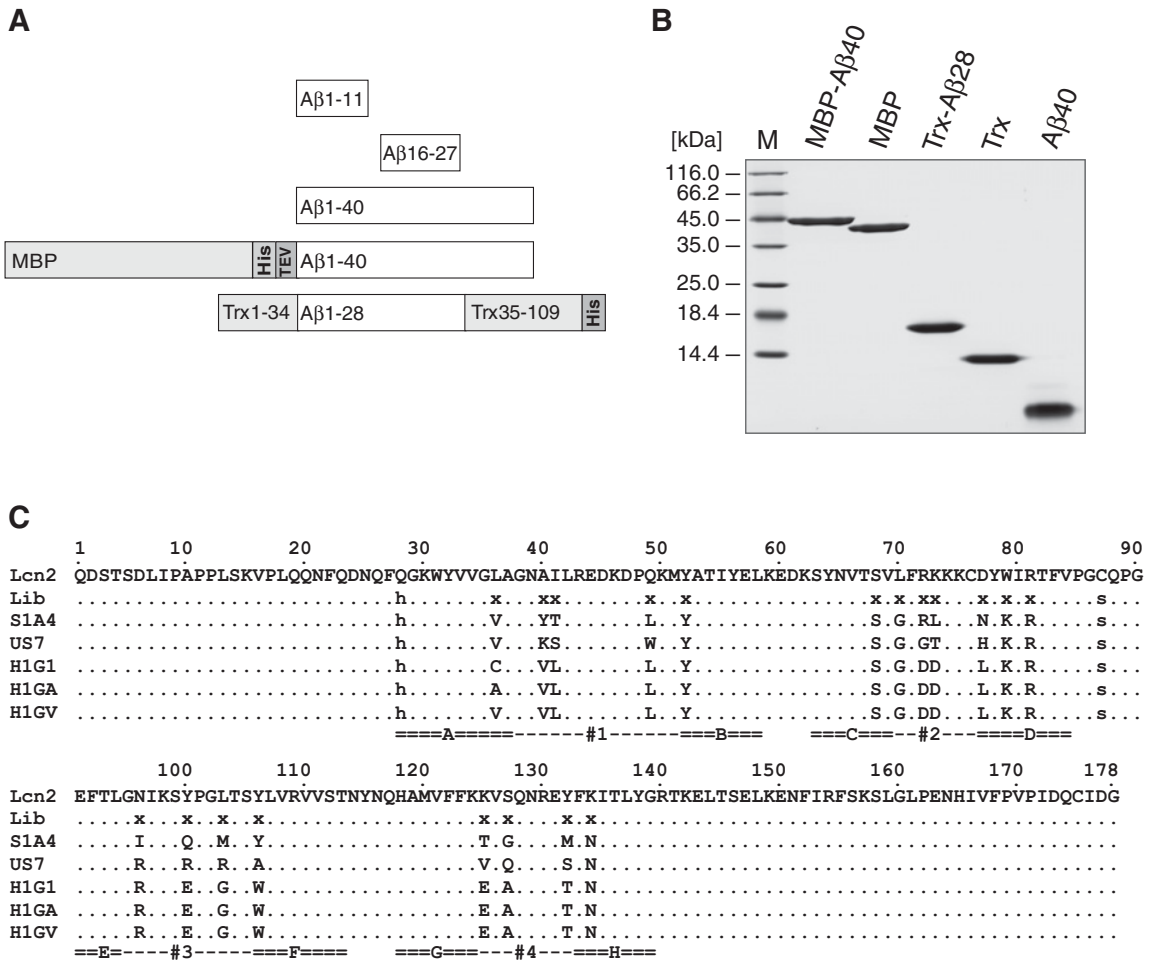

Figure 1 Preparation of Aβ target peptides and amino acid sequences of selected Aβ-specific Anticalins

(**A**) Schematic overview of the different Aβ targets used for selection and characterization of cognate Lcn2 variants. Peptides corresponding to the full length 40mer (Aβ40) or shorter versions, such as the N-terminal (Aβ1–11) and central (Aβ16–27) fragment, were obtained by chemical synthesis. Aβ40 was also prepared in the form of recombinant fusion proteins, either with the *E. coli* MBP (MBP-Aβ40) or as a hybrid with *E. coli* TrxA carrying the Aβ1–28 moiety inserted into its active site loop (Trx-Aβ28), both also comprising a His_6-tag for affinity purification. (**B**) Analysis of monomeric Aβ target proteins by SDS/15 % PAGE. The Aβ fusions and control proteins were expressed in the cytoplasm of *E. coli* and purified via IMAC and SEC. Aβ40 corresponds to the synthetic peptide treated with HFIP and dissolved in H_2O (see Materials and Methods). M is the molecular size marker. (**C**) Amino acid sequences of selected Aβ-specific Lcn2 variants. Randomised positions in the library (Lib) are labelled with x whereas fixed amino acid exchanges are marked by lower case letters [34]. Dots represent amino acids identical with the wtLcn2 sequence (SWISS-PROT entry P80188). The eight structurally conserved β-barrel strands A–H and the four structurally hypervariable loops #1–#4 that form the binding pocket are labelled. Cys^{76} and Cys^{175} form a disulfide bridge.

flask and at the bench top fermenter scale, followed by affinity purification via the C-terminal *Strep*-tag II as well as SEC. All Lcn2 variants were obtained in a pure homogeneous state as judged by SDS/PAGE (Supplementary Figure S2).

S1A4 and US7 showed particularly high yields of more than 200 mg purified protein from an 8 litre fed-batch fermenter and predominantly monomeric state as revealed by SEC (Supplementary Figure S2A). However, the third candidate, H1G1, was produced at a much lower yield, with approximately 40 mg under the same conditions, and exhibited a tendency to aggregate. This behaviour was attributed to a single free thiol side chain that occurred at one of the mutated positions (Cys^{36}).

Therefore, we decided to exchange the unpaired Cys residue in this Anticalin either by Ala (C36A: dubbed H1GA), as inert side chain, or by Val (C36V: dubbed H1GV), because the other two selected Anticalins carried the same residue at this position (cf. Figure 1C). Both amino acid substitutions abolished aggregation, resulting in purely monomeric protein as judged by SEC. In addition, production as soluble protein was much improved, with 8.4-fold (H1GA) and 15-fold (H1GV) increased yields when expressed in a 2 litre shake flask culture. Unexpectedly, as a further benefit, the affinity to Aβ40 measured via surface plasmon resonance (SPR) was considerably improved by 70-fold and 20-fold respectively, as described further below.

To analyse folding stability, thermal melting curves of the Aβ-specific Anticalins in comparison with the recombinant wild-type (wt) Lcn2 protein were recorded via CD spectroscopy (Supplementary Figures S2C and S2D). Similar to wtLcn2, all selected Anticalins denatured according to a simple two-state model of cooperative unfolding, allowing data fitting by means of the integrated van't Hoff equation [52]. H1GV exhibited a remarkably high T_m value of 73.0 °C, just slightly less stable than the wtLcn2 scaffold (T_m = 78.6 °C), followed by H1GA, US7, and S1A4 with T_m values of 66.2, 59.6 and 53.4 °C respectively (Supplementary Table S1). Notably, despite the unpaired thiol side chain, H1G1 exhibited the highest thermal stability among the selected Anticalins, with a T_m value of 74.5 °C.

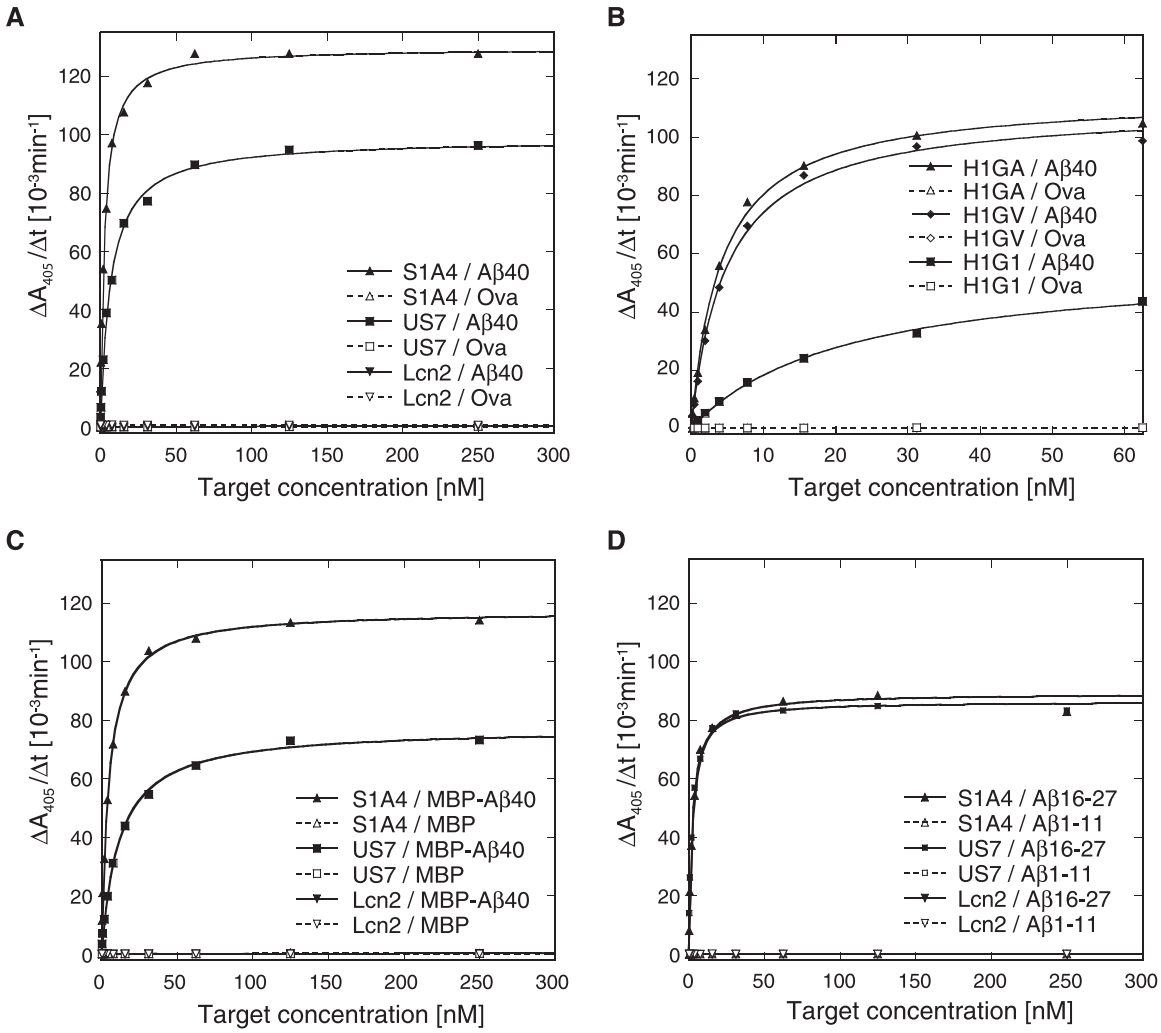

Figure 2 Affinity analysis of Aβ-specific Anticalins by ELISA

Binding activity was analysed in a capture ELISA for the biotinylated full-length Aβ40 (**A**, **B**) and MBP-Aβ40 (**C**) as well as for the short biotinylated peptides Aβ1–11 and Aβ16–27 (**D**). The purified Anticalins were immobilized on to microtitre plates via the *Strep*-tag II specific antibody *Strep*MAB-Immo and incubated with a dilution series of the biotinylated Aβ targets (filled symbols) or control proteins (empty symbols), i.e. ovalbumin (Ova) and the MBP. Bound targets were subsequently detected with an ExtrAvidin-Alkaline Phosphatase conjugate, followed by a chromogenic reaction. All Anticalins showed specific binding of the full-length Aβ targets in the low nanomolar range (for the Trx-Aβ28 target cf. Supplementary Figure S3). In addition, there was detectable binding activity towards the central peptide Aβ16–27, but not towards the N-terminal peptide Aβ1–11, as shown here for S1A4 and US7.

Affinity analysis and epitope specificity of Aβ-specific Anticalins

The synthetic and recombinant Aβ target peptides described above were used to systematically investigate binding activity and sequence specificity of the selected Anticalins by ELISA (Figure 2; Supplementary Figure S3). First, a capture ELISA was performed wherein purified Lcn2 variants were selectively immobilized via an anti-*Strep*-tag II antibody on to a microtitre plate and probed with the biotinylated targets. These measurements revealed pronounced binding activity of all Lcn2 variants (H1G1, H1GA, H1GV, S1A4 and US7) towards the synthetic Aβ40 peptide, irrespective of the differing strategies that had been applied during phage display selection (Figures 2A and 2B). Likewise, the recombinant fusion proteins MBP-Aβ40 (Figure 2C) and Trx-Aβ28 (Supplementary Figures S3A and S3B) were bound with apparent dissociation constants (K_D) in the low nanomolar range (Supplementary Table S2). In contrast, no binding activity was detected for wtLcn2 with any of the Aβ target molecules tested.

Binding kinetics of the Lcn2 variants were investigated by real-time SPR analysis (Figure 3, Supplementary Figure S3C) using immobilized synthetic Aβ40 peptide and, for comparison, recombinant MBP-Aβ40. All Lcn2 variants exhibited fast and tight binding to both Aβ targets with K_D values in the low nanomolar down to the picomolar range (Table 1), in line with the previous ELISA results. However, despite their similar K_D values, especially S1A4 and US7 differed markedly in their k_{on} and k_{off} values. Interestingly, the single substitution C36A introduced into H1G1 (yielding the variant H1GA) resulted in an improved affinity towards Aβ40 by about 70-fold, whereas the corresponding mutation C36V showed a 20-fold improvement. For H1GA, an increase in k_{on} by a factor of approximately 24 and a lower k_{off} by a factor 3 was responsible for the much better K_D value of 95 pM. Accurate determination of the slow k_{off} rate of H1GA on a Biacore T100 instrument, with extended measurement of the dissociation phase, indicated a remarkably long half-life of $\tau_{1/2} = 16$ h for the complex between this Anticalin and the Aβ40 peptide.

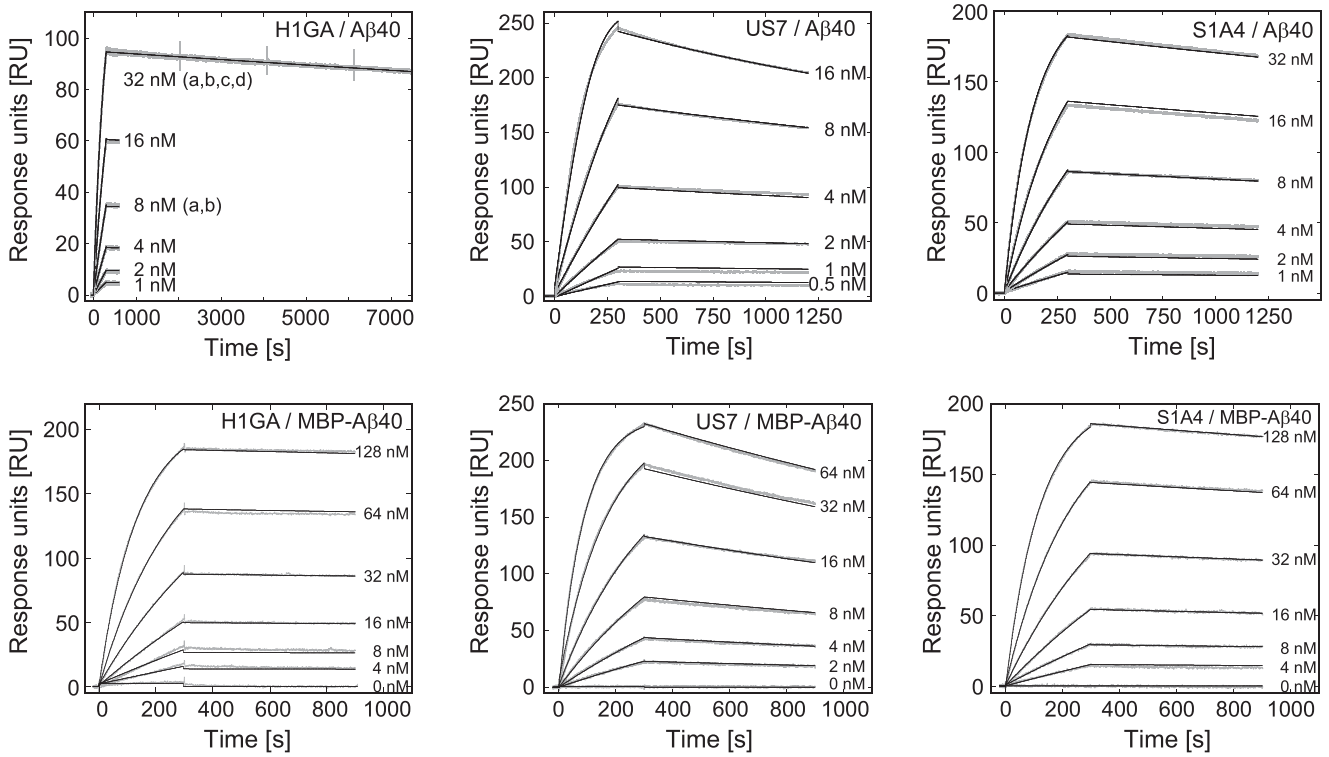

Figure 3 Real-time kinetic analysis of Aβ binding by Anticalins via SPR

The synthetic Aβ40 peptide was covalently immobilized on to a CM5 sensor chip, with $\Delta RU = 325$, using amine coupling chemistry and the purified Lcn2 variants were applied at a flow rate of 30 μl/min. The recombinant MBP-Aβ40 fusion protein was similarly immobilized at a ligand density of $\Delta RU \approx 1300$ RU and Lcn2 variants were applied at a flow rate of 20 μl/min. The measured sensorgrams (grey lines) were corrected twice, i.e. by subtraction of the corresponding signals measured for the control channel and of the average of three buffer injections. k_{on} and k_{off} parameters were globally fitted using a 1:1 Langmuir binding model (black lines). For exact determination of the low k_{off} rate of H1GA the highest concentration was repeatedly analysed using a prolonged dissociation time of 7200 s. The kinetic parameters and dissociation constants are summarized in Table 1 for all investigated Anticalins (for additional SPR sensorgrams cf. Supplementary Figure S2).

Table 1 Affinity and kinetic data determined for anti-Aβ Anticalins in SPR measurements

*Dissociation time was insufficient to determine an accurate dissociation rate for the MBP-Aβ40 complex.

	Aβ40				MBP-Aβ40			
	k_{on} [10^5 $M^{-1}\cdot s^{-1}$]	k_{off} [10^{-5} s^{-1}]	K_D [nM]	$\tau_{1/2}$ [min]	k_{on} [10^5 $M^{-1}\cdot s^{-1}$]	k_{off} [10^{-5} s^{-1}]	K_D [nM]	$\tau_{1/2}$ [min]
S1A4	2.30 ± 0.001	9.06 ± 0.03	0.394 ± 0.0013	128	0.652 ± 0.001	8.41 ± 0.08	1.29 ± 0.012	137
US7	10.8 ± 0.03	24.1 ± 0.05	0.223 ± 0.00077	48	1.71 ± 0.001	31.8 ± 0.1	1.86 ± 0.0059	36
H1G1	0.0432 ± 0.0001	5.17 ± 0.14	12.0 ± 0.33	223	0.0300 ± 0.0002	4.74 ± 0.09	15.8 ± 0.32	244
H1GA*	1.25 ± 0.001	1.19 ± 0.001	0.095 ± 0.00011	971	–	–	–	–
H1GA	1.04 ± 0.001	1.70 ± 0.11	0.163 ± 0.011	680	0.577 ± 0.001	2.75 ± 0.13	0.476 ± 0.023	420
H1GV	0.997 ± 0.001	5.61 ± 0.10	0.563 ± 0.010	206	0.684 ± 0.001	7.26 ± 0.18	1.06 ± 0.026	159

To narrow down the epitope recognized by the Aβ-specific Anticalins S1A4 and US7 a capture ELISA was performed with the shorter N-terminal and central peptide fragments, Aβ1–11 and Aβ16–27 respectively (Figure 2D). Both S1A4 and US7 appeared to bind Aβ16–27 with affinities in the low nanomolar range (Supplementary Table S2), similar to the full length Aβ40 peptide, but not Aβ1–11, indicating specific recognition of a central epitope within the amyloid peptide. For more detailed analysis, a residue-wise epitope mapping was conducted utilizing the SPOT technique [55] (Figure 4). In this manner, the minimal sequential epitope on Aβ40 that governs binding by US7 was identified as the amino acid sequence $F^{19}FAED^{23}$ (Figure 4, US7). Interestingly, the epitope for S1A4 matched exactly the same sequence (Figure 4, S1A4) whereas H1G1 seemed to recognize a slightly shifted epitope including the preceding Val residue (Figure 4, H1G1).

Anticalins inhibit Aβ40 aggregation at sub-stoichiometric concentrations and prevent Aβ42 fibril formation *in vitro*

The ability of the selected Anticalins to interfere with Aβ aggregation *in vitro* was assessed using ThT as a probe for β-sheet amyloid fibril formation [60]. To this end, the aggregation kinetics of the freshly solubilized synthetic Aβ40 peptide (adapted from [5]) was monitored via ThT fluorescence in the presence of different molar ratios of each Anticalin – or some dummy proteins such as wtLcn2 or BSA (Figure 5). Generally, the observed

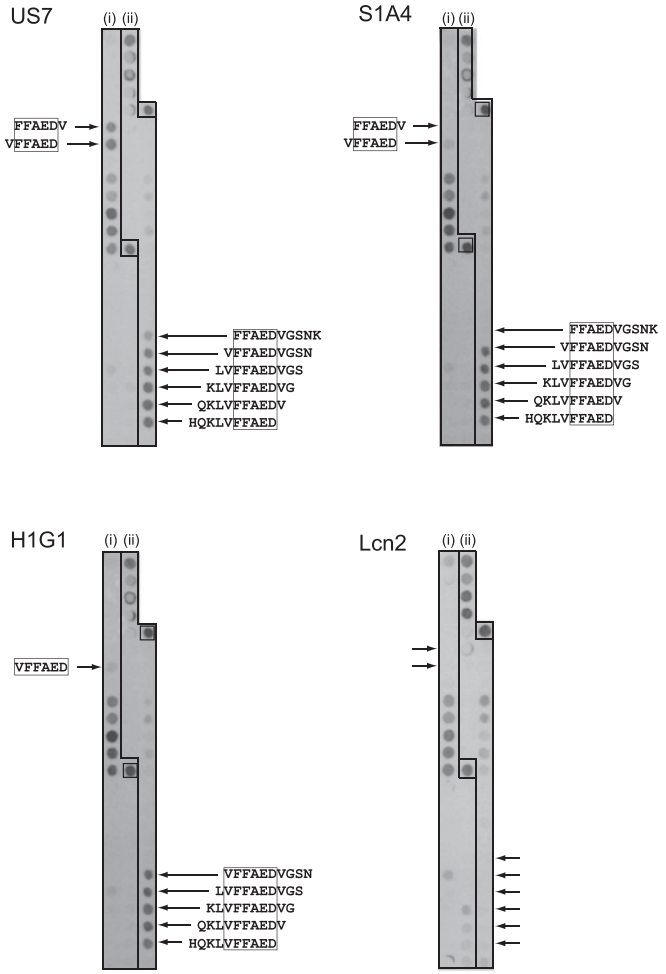

Figure 4 The epitopes of the Aβ-specific Anticalins were localized by mapping on a SPOT membrane

The entire amino acid sequence of Aβ40 was synthesized as consecutive hexamer (i) and decamer peptides (ii), each with a dislocation of 1 residue, on a hydrophilic cellulose membrane. The membrane strips were incubated with the selected Anticalins, followed by detection via the *Strep*-tag II. The synthetic *Strep*-tag II peptide itself was present on the same membrane as a positive control (box). Neglecting non-specific background signals that were also seen for wtLcn2, the motif FFAED – corresponding to positions 19–23 of Aβ40 – appeared as the minimal epitope sequence of the Anticalins US7 and S1A4. H1G1 recognized a related epitope which also covered the preceding Val residue (VFFAED).

aggregation kinetics showed a characteristic sigmoidal shape corresponding to phases of Aβ nucleation, aggregate growth and saturation and/or maturation, in line with previous studies [61]. The data were best fitted to an autocatalytic reaction model for β-amyloid aggregation kinetics [57] (see Materials and Methods).

Notably, at equimolar concentrations (231 μM) of Anticalin and Aβ40 all tested Lcn2 variants completely suppressed Aβ fibril formation during the entire duration of the experiment (3 h). This indicates efficient sequestration of Aβ monomers – or, possibly, prenuclear oligomeric intermediates – via bimolecular complex formation, in agreement with the tight binding activity of the Anticalins described above. In contrast, wtLcn2 or BSA had no significant influence on Aβ aggregation in this assay. In fact, Aβ40 without any added protein showed a similar nucleation rate as in the presence of wtLcn2. If the Anticalins were applied at lower, sub-stoichiometric concentrations, a significant decrease in the values of the nucleation rate k_n in comparison with the control reaction was still observed (Supplementary Figure S4 and Table S3), and Aβ aggregation propensity was decreased in a both dose-dependent and individual manner for each variant (Figure 5).

H1GA (Figure 5A) had the strongest inhibitory activity of all Anticalins tested and was able to significantly mitigate aggregation even at a rather low Anticalin:Aβ ratio of 20:100. H1GV (Figure 5B), S1A4 (Figure 5C) and US7 (Figure 5D) clearly retarded Aβ40 aggregation at a sub-stoichiometric molar ratio of 50:100. Interestingly, US7 revealed a somewhat peculiar behaviour by strongly hampering nucleation already at a molar ratio of 20:100 but then evoking a higher amplitude of Aβ aggregation towards the saturation phase.

It is well known that freshly formed Aβ oligomers/aggregates undergo a maturation process called 'aging' [6,62], which depends on time and incubation conditions (such as temperature and peptide concentration), finally resulting in the generation of fibrils. The influence of the selected Anticalins on fibril formation was investigated by TEM using synthetic Aβ42 preparations (see Materials and Methods and Supplementary Figure S5). Indeed, strong fibril formation was observed for Aβ42 alone upon incubation at 37 °C for 72 h. In contrast, fibrils were almost absent from fresh peptide preparations and their formation was hardly recognisable after incubation under less harsh conditions at 4 °C for 6 h (data not shown), in line with previous reports [63].

To investigate the effect of Anticalins on fibril formation, Aβ42 was initially incubated for 6 h at 4 °C and, after addition of the Aβ-specific Anticalins – or control proteins – this mixture was further incubated at 37 °C for 72 h (Figure 6). At equimolar concentrations of Aβ42 and Anticalin, S1A4, H1G1, H1GA and H1GV almost completely suppressed fibril formation, very similar to the inhibitory effect seen here for the anti-Aβ antibody 6E10 [64], which was included as a positive control. wtLcn2 affected fibril formation to a minor extent; it did not prevent formation of oligomeric protofibrillar Aβ species. Also, Anticalins themselves did not generate fibrils under any condition tested (Supplementary Figure S5B).

Anticalin-mediated protection against cytotoxic effects of Aβ42 oligomers in neuronal cell culture

Incubation of NGF-β differentiated PC12 cells, which exhibit a neuronal phenotype, with 10 μM 'aged' Aβ42 peptide at 37 °C for 72 h caused approximately 77 % cellular death as measured by a metabolic MTT assay [65,66] (Figures 6B and 6C). To this end, we performed the Aβ42 aging process under less harsh conditions, at 4 °C for 6 h as described above, to ensure the primary formation of sufficient amounts of cytotoxic oligomers – instead of the less toxic fibrils, which would predominantly occur at higher temperatures and longer incubation times.

To investigate the protective effect of different Anticalin candidates on Aβ-mediated cytotoxicity, aged Aβ42 was incubated with each Anticalin at various molar ratios Anticalin:Aβ42 of 10:10, 5:10 or 2:10 (μM). As a result, a concentration-dependent suppression of the cytotoxic Aβ42 effect in the following order was observed: S1A4 $\geqslant$ H1G1 > H1GA > US7 $\gg$ wtLcn2. Notably, both Anticalins H1G1 and S1A4 prevented Aβ42-mediated cytotoxicity almost completely when added at equimolar concentrations (i.e. at 10 μM) while H1GA showed approximately 50 % less protective capacity at the same ratio.

The Anticalins alone just showed minor effects on neuronal cell viability (Supplementary Figure S5C) with the only exception being the US7 preparation, which caused cellular death up to nearly 40 %. As this result was dose-dependent and declined with

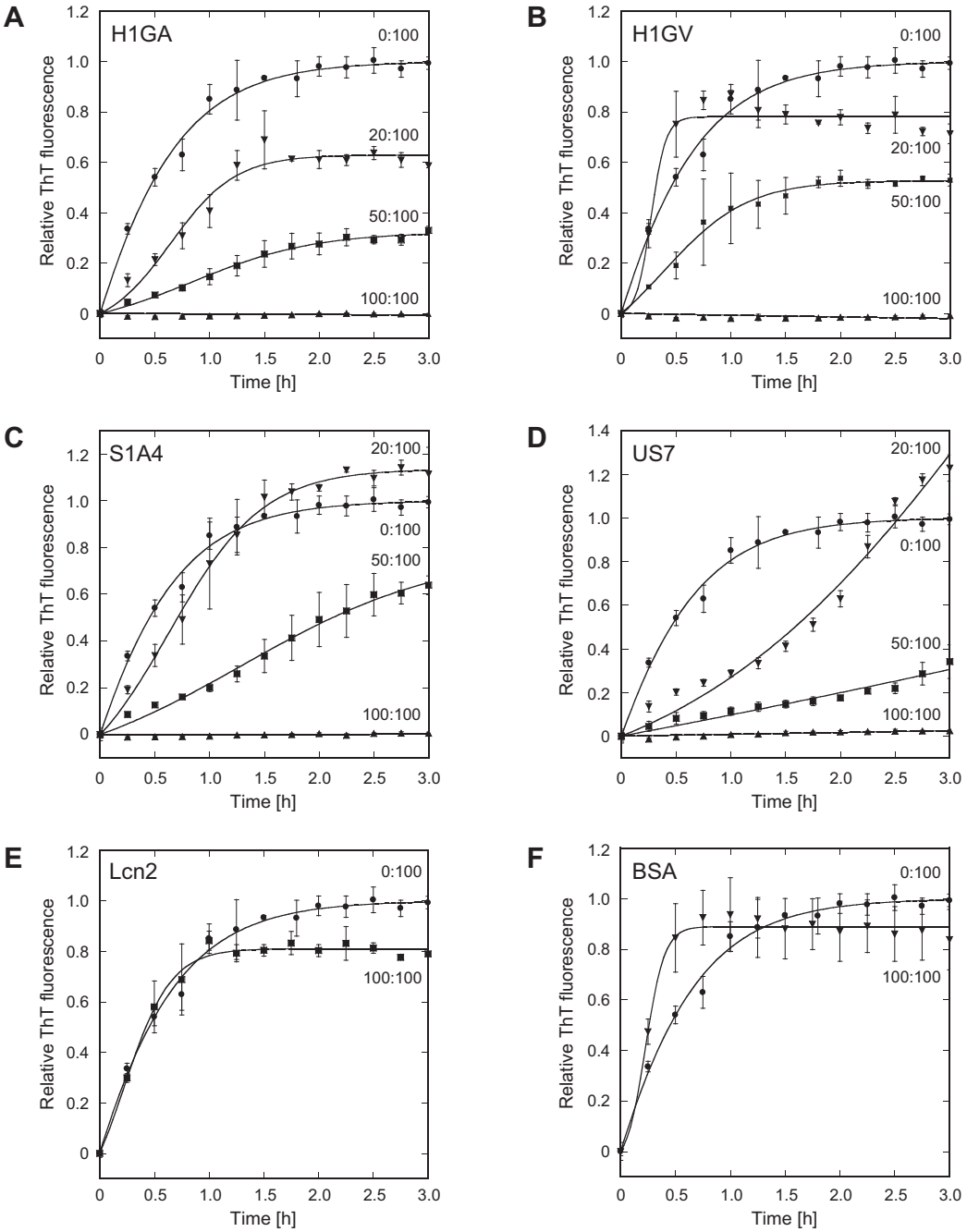

Figure 5 Effect of Anticalins on Aβ40 aggregation *in vitro*

The influence of H1GA (**A**), H1GV (**B**), S1A4 (**C**) and US7 (**D**) on the aggregation kinetics of the Aβ40 peptide – freshly dissolved in doubly distilled cold H_2O – was monitored via ThT fluorescence. Monomeric Aβ40 (1 mg/ml) was incubated at 37 °C with agitation in the absence or presence of Anticalins using different molar ratios (given as percentages) in PBS. Small samples were periodically removed, mixed with ThT and analysed for fluorescence (λ_{em} = 450 nm; λ_{ex} = 482 nm). The data were averaged from multiple, independent experiments ($n = 3$, error bars indicate standard deviations) and fitted to a model for an autocatalytic reaction (see Materials and Methods). In contrast with the mock proteins wtLcn2 and BSA (**E**, **F**), equimolar amounts of all selected Anticalins inhibited Aβ aggregation completely. Even at lower molar ratios aggregation propensity was reduced in a dose-dependent manner, yet with varying curve shapes.

lower US7 concentrations (data not shown) this effect was likely due to contaminations from the recombinant protein production in *E. coli*. However, application of wtLcn2 revealed no cytotoxic effect at all, which in combination with the strong persistent effects mediated by Aβ42 itself, convincingly supported specific neuronal cell-protective activities of the selected Anticalins.

DISCUSSION

In the present study we have developed novel binding proteins for the Alzheimer amyloid-β peptide based on the human lipocalin scaffold (Lcn2). Conceptually, we anticipated that Anticalins directed against linear epitopes on soluble Aβ peptides would recognize nascent monomeric or early oligomeric states of both

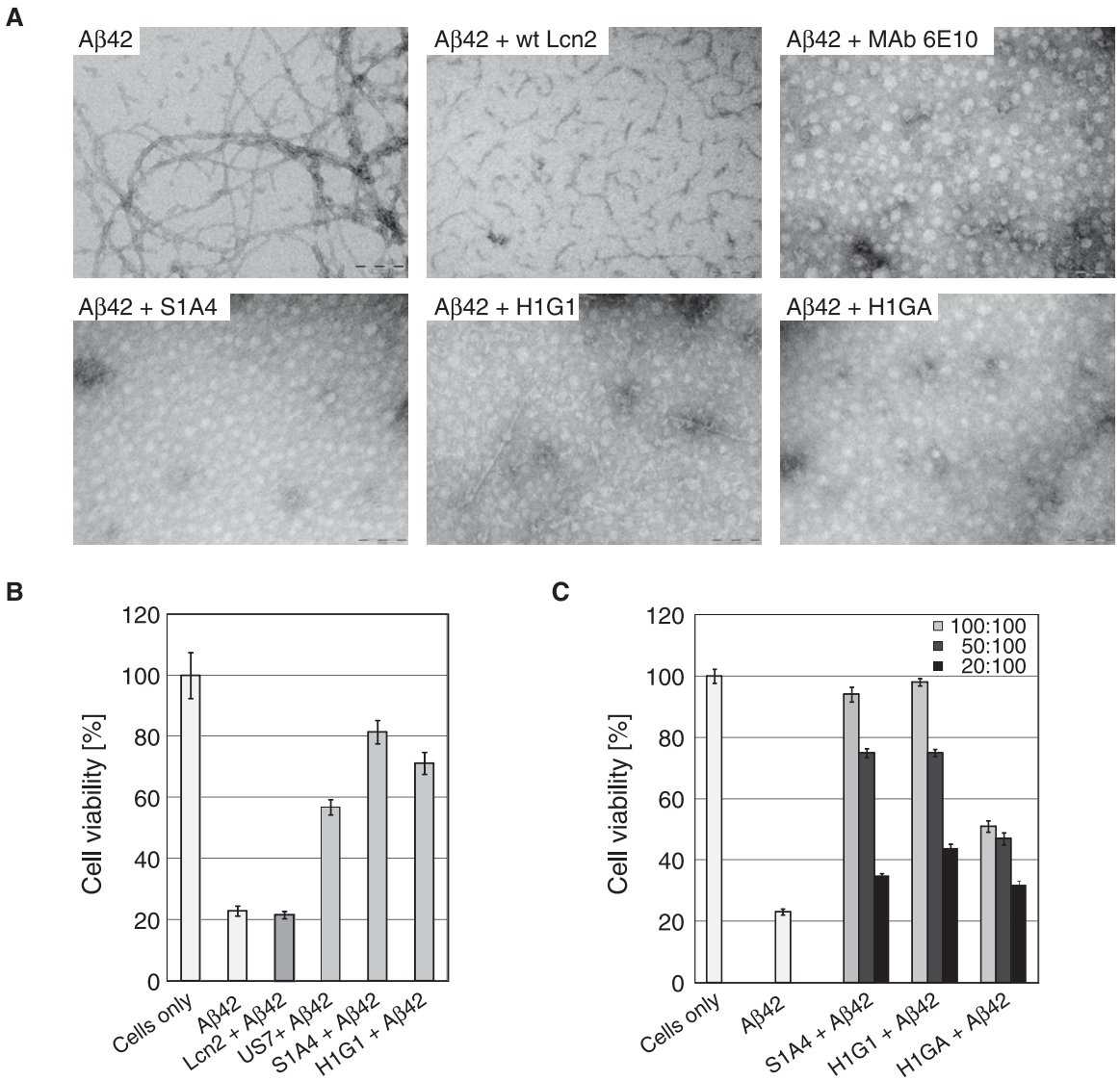

Figure 6 Effect of Anticalins on Aβ42 fibril formation and neuronal cytotoxicity

(**A**) Macromolecular fibril formation was monitored via TEM starting from Aβ42 dissolved at 200 μM (0.9 mg/ml) in 5 mM NaOH. Subsequently, 1 volume of 20 mM Tris/HCl, pH 6.8 was added by vortex-mixing. The solution was then incubated at 4 °C for 6 h without agitation, prior to dilution in RPMI-1640 cell culture medium to a final concentration of 10 μM. Aβ42 alone or in combination with equimolar concentrations of wtLcn2 (negative control), MAb 6E10 (positive control) or the Aβ-specific Anticalins S1A4, H1G1 and H1GA were incubated at 37 °C for 72 h and then subjected to TEM. (**B**, **C**) The toxicity of Aβ42 alone or in combination with Anticalins on NGF-β differentiated PC12 cells was analysed in an MTT reduction assay. (**B**) Aβ42 was preincubated at 4 °C for 6 h in a mixture of 1 volume 5 mM NaOH and 1 volume 20 mM Tris/HCl, pH 6.8 and then added at a concentration of 10 μM alone or in combination with equimolar concentrations of the Lcn2 variants to the cells. wtLcn2, S1A4 and H1G1 alone (without Aβ42) showed only minor cytotoxicity (see Figure S5C in the supplementary data section). (**C**) Anticalins with promising effects (H1GA not shown) were further analysed for their potential to support cell viability up to stoichiometric ratios in the presence of 10 μM Aβ42 (measured as in B). For each experiment, measurements of replicates were derived from different wells ($n = 4$–8) of a single 96-well plate from which the median was calculated. Several plates were measured on different days as independent experiments for cell viability ($n \geqslant 3$) from which the mean was calculated. Error bars represent standard deviations of the means.

Aβ40 and Aβ42, the two predominant pathological species [67], including versions with N-terminal modifications such as pyroglutamate [68]. Thus, such protein reagents should both be compatible with scavenging Aβ in the circulation, in line with the peripheral sink hypothesis [18], and, possibly, even be able to prevent Aβ aggregation via complex formation directly in the brain tissue (ideally, prior to onset of the disease).

According to the amyloid hypothesis [6], changes in the biosynthesis and/or metabolism of Aβ peptides, especially their aggregation into oligomers, elicit a pathophysiological cascade that eventually leads to neurodegenerative disorders such as, in particular, AD. The peripheral sink hypothesis implies that a systemically administered anti-Aβ antibody may shift the dynamic equilibrium between monomeric Aβ in the brain interstitial fluid and in the blood plasma [18]. Consequently, sequestration of the soluble peptide in the periphery may stimulate Aβ efflux from the central nervous system and effect reduced amyloid burden in the brain. Since according to this biomedical mechanism no passage of the Aβ-binding agent across the BBB is required and, furthermore, immunological effector functions do not play a role, Anticalins with their high specific binding capacity,

small size and robust nature provide an attractive alternative to conventional therapeutic antibodies.

Here, we succeeded in selecting from a new Lcn2-based random library three different Aβ-specific Anticalins (S1A4, US7, H1G1) having low to sub-nanomolar affinities, notably without an affinity maturation step as in previous Anticalin selection studies [33]. Alternative binding proteins based on different scaffolds with specificity for Aβ were previously selected using phage display or ribosomal display, i.e. an affibody molecule [24,25] and a DARPin [26], but had clearly lower affinities: K_D values were 17 nM for the (dimerized) affibody molecule as determined by isothermal titration calorimetry and 158 nM for the monomeric DARPin as determined by SPR. This confirms the superior design of our new Anticalin library, which allows the selection of high-affinity binders both for macromolecular protein targets [34] as well as for small molecule ligands including peptides [27].

Replacement of an unpaired Cys residue in the Aβ-specific Anticalin H1G1 led to two particularly potent variants (H1GA and H1GV) that showed improved expression characteristics and even stronger target affinity (95 pM and 560 pM respectively). Periplasmic expression in *E. coli* and subsequent purification of all selected Lcn2 variants was feasible with high yields. Furthermore, size exclusion chromatography demonstrated the strictly homogenous monomeric nature of these small proteins (21 kDa) whereas CD measurements revealed high thermal stability, which is an important benefit for therapeutic protein development.

Apart from antibodies, several engineered binding proteins with specificities for different forms of the amyloid-β peptide have been generated during recent years [69]. These protein reagents appear useful for the detection, diagnosis or imaging of Aβ or amyloid deposits and could even offer potential as novel therapeutics for the treatment of AD. The two Aβ-specific V_HH domains B10 [22] and KW1 [23] as well as the atypical dimeric Affibody $Z_{A\beta3}$ [24,25] were selected via phage display using Aβ40 fibrils, Aβ40 oligomers or monomeric Aβ40 respectively. In contrast, the DARPin D23 [26] was generated using ribosomal display with the biotinylated truncated Aβ fragment Aβ(1–28) to enable selection of binders against the soluble, monomeric Aβ peptide. All these engineered proteins showed *in vitro* inhibition of amyloid aggregation to various extents. In addition, continuous intracerebroventricular infusion of D23 led to improved cognition in APPswe transgenic mice. Also, $Z_{A\beta3}$ coexpression abolished the neurotoxic effect of Aβ in a *Drosophila melanogaster* animal model transgenic for both Aβ42 and the Affibody [70]. Surprisingly, the Aβ oligomer-specific V_HH domain KW1 did not show a comparable beneficial effect in Aβ40-transgenic *Drosophila* flies but even provoked toxicity, despite its ability to antagonize synaptotoxicity of pre-formed Aβ40 oligomers *in vitro* [71].

Interestingly, while using different Aβ targets in the present study for the phage display selection of the three Anticalins, and in spite of their considerable sequence differences in the binding site, all of them are directed against the same epitope in the mid-region of Aβ, namely (V)FFAED (residues P18/19–P23). Notably, according to previous studies the hydrophobic VFF stretch within the central KLVFF motif seems to play a major role in the process of amyloid aggregation [72,73]. Furthermore, specific mutations in this region – which is located in the vicinity of the α-secretase cleavage site [74] – are attributed to rare hereditary forms of AD [75]; these appear to affect Aβ conformation, oligomerization and/or fibrillation propensity and often cause the phenotype of cerebral amyloid angiopathy (CAA) [76]. For example, the mutations E22Q (Dutch; [77]), E22K (Italian; [78]) and D23N (Iowa; [79,80]) result in an increased rate of amyloid fibrillation, whereas the mutation A21G (Flemish; [81]) causes elevated amounts of Aβ40 and Aβ42, most likely due to interference with α-secretase processing. Finally, the mutation E22G (Arctic; [76]) leads to strongly increased formation of protofibrils and causes the early onset of a classical phenotype of AD.

Further studies suggest that residues in the segments P18–P26, and also P31–P42, play a pivotal role for Aβ42 aggregation into fibrils [82]. It has been proposed that these regions are part of two antiparallel intramolecular β-strands in an intermediate state of monomeric Aβ. This β-hairpin is believed to undergo a conformational transition, eventually forming multiple stacked intermolecular parallel in-register β-strands as part of the extended amyloid fibril [25]. Hence, it seems that the Anticalins do not only sterically prevent Aβ peptides from oligomerization via complex formation but also functionally block a conformationally critical region that plays a crucial role in the mechanism of oligomerization and fibril assembly.

Position PhePP19 within the epitope recognized by the Anticalins seems to be especially important for stabilization of Aβ intersheet interactions [82]. Indeed, in several amyloid-related peptides such conserved aromatic residues promoted fibril self-assembly via $\pi-\pi$ stacking interactions [83]. A role for intersheet stability in Aβ fibrils was also discussed for the AspP23–LysP28 salt bridge [82]. In line with these observations, several groups have successfully designed short peptide mimetics which either encompass [84] or resemble [85] the central hydrophobic LVFF motif of the Aβ peptide and can inhibit conversion of monomeric peptide into β-sheet-rich aggregate structures.

We could demonstrate that the Anticalins H1GA/H1GV, S1A4 and US7 effectively suppress Aβ aggregation *in vitro*, which is in agreement with previous findings that antibodies directed against the central region of Aβ are able to inhibit Aβ fibrillation [86]. Furthermore, at equimolar ratios between Aβ and each of these Anticalins, complete inhibition of aggregation was observed in a ThT fluorescence assay. In particular, H1GA exhibited the strongest inhibitory effect among the tested Anticalins, in accordance with its unrivalled target affinity. Dose-dependent retardation or partial inhibition of aggregation could be demonstrated down to a submolar ratio of 20:100 for H1GA as well as at ratios of 50:100 for H1GV, S1A4 and US7. Importantly, neither the wild-type lipocalin nor dummy proteins such as BSA influenced Aβ aggregation substantially in this experimental setup.

It is known that the initial lag time for Aβ nucleation is reciprocally proportional to the free peptide concentration [57]. According to the Law of Mass Action the presence of an equimolar concentration of the Aβ-specific Anticalin considerably reduces the effective concentration of free monomeric Aβ40 that is available for nucleation, depending on the dissociation constant of the complex. Compared with that, even though the proportion of free Aβ40 is not much decreased when applying the Anticalin at sub-stoichiometric ratio, Aβ nucleation was still substantially retarded for all Anticalins tested. This supports the notion that the Anticalins may recognize a critical conformation of the Aβ peptide on the path toward oligomer formation. Interestingly, a similar observation was made with the Aβ-specific dimeric Affibody, which led to complete inhibition of Aβ aggregation when applied in 1.1 molar equivalents [25]. In contrast, the Aβ-specific DARPin showed only a delay and reduction in overall fluorescence in the ThT assay but no complete inhibition of aggregation when applied at equimolar concentration [26].

The efficacy of the Anticalins with regard to protecting neuronal cell viability in the presence of 'aged' oligomeric Aβ42 was assessed in cell culture using a metabolic assay.

Indeed, a protective effect against Aβ-mediated cytotoxicity could be demonstrated for all three Anticalins, most pronounced for S1A4 and H1G1. Unexpectedly, this effect was less evident for H1GA, which showed the highest affinity for soluble Aβ40 among the selected Lcn2 variants as well as the strongest inhibitory effect on Aβ aggregation. H1G1, its predecessor with only one amino acid exchange, was able to potently suppress Aβ-mediated cytotoxicity in a dose-dependent manner. Possibly, this distinct behaviour of the Aβ-specific Lcn2 variants selected here reflects subtle differences in the way conformational states of the target peptide are recognized.

Previously described anti-Aβ antibodies directed against the N-terminal and central regions of the peptide were shown to decrease amyloid plaques in the brain either via Fc-mediated phagocytosis or according to the peripheral sink mechanism [87]. Accordingly, the two humanized monoclonal antibodies Bapineuzumab and Solanezumab, which recognize N-terminal and central epitopes in the Aβ peptide respectively, were the first antibodies to be investigated in Phase III clinical trials [88,89]. Unfortunately, both antibodies failed to meet their primary endpoints to treat AD in these large studies, which has to be attributed to the late initiation of treatment in the patient population after clinical symptoms had already emerged.

Based on the notion that therapies targeting amyloid-β should start early on in order to allow modification of disease progression, a secondary subgroup analysis taking into account disease severity was performed on the results of the Solanezumab Phase III trials EXPEDITION and EXPEDITION2 [90]. This analysis revealed that in patients with mild AD, as opposed to moderate AD, treatment with Solanezumab resulted in a slowing of the cognitive decline by approximately 34 % and slowing of the functional decline by approximately 18 %. Increases in plasma and total CSF (bound and unbound) Aβ additionally indicated target engagement by Solanezumab in the periphery and the central nervous system. Justified by these data a new Phase III study (EXPEDITION3) was initiated exclusively in patients at this early pathological state [91].

It is well established that some Alzheimer biomarkers, such as the deposition of amyloid-β in the brain, can precede symptomatic dementia by up to 20 years [92,93] and that antibody treatment has to be started before first symptoms occur. Hence, three initiatives are currently underway to investigate the efficacy of monoclonal antibodies when administered in a preventive setting [94]: (i) the A4 trial, anti-amyloid treatment for asymptomatic AD, (ii) the DIAN trial, the Dominantly Inherited Alzheimer Network, and (iii) the API trial, the Alzheimer Prevention Initiative. Lilly's Solanezumab and Genentech's Crenezumab, which target the same epitope on Aβ (P13–P28) and show high mutual homology in their CDRs [95], are two of the antibodies tested in these prevention trials.

By targeting a central epitope of Aβ comparable to the one recognized by Solanezumab and Crenezumab we expect that the Anticalins reported here will prove valuable for future *in vivo* studies such as in mouse models of AD. Notably, Solanezumab targets the soluble Aβ peptide and is proposed to act according to the peripheral sink hypothesis as was shown for the mouse version of this antibody, m266 [18,96]. Aβ engagement both in the periphery and the central nervous system was confirmed in the clinical trials by a measurable increase in total Aβ content in plasma and cerebrospinal fluid [89,90,97]. Considering that lipocalins naturally serve for the transport and scavenging of pathological substances in body fluids – e.g., Lcn2/NGAL scavenging bacterial siderophores – the selected Anticalins appear promising for application to clear Aβ peptides from blood and brain according to the peripheral sink mechanism, too. Since Anticalins lack an Ig Fc region, the risk for deleterious inflammatory responses, especially antibody-mediated microhaemorrhages and vasogenic oedema [98], should be much less than with antibodies either during active or passive immunization.

Furthermore, the much lower molecular mass of the Anticalins in comparison with monoclonal antibodies should allow for lower dosing when used to treat AD patients. A mode of action according to the peripheral sink hypothesis, as suggested for Solanezumab, means that the therapeutic protein needs to be administered at least in stoichiometric amounts of circulating Aβ in order to achieve full complexation. Compared with a molecular mass of 72.2 kDa per mole equivalent of the bivalent antibody the Anticalins have a mass of approximately 21.5 kDa, that is less than one third – while showing similar affinities in the low nanomolar to subnanomolar range – hence offering a clear benefit. Also, the shorter plasma half-life of Anticalins should allow more rapid renal clearance of complexed Aβ peptide from blood and avoid accumulation of a circulating depot. Finally, by employing modern targeted delivery systems such as receptor-mediated transport via the BBB [99,100], Anticalins may even be actively translocated into the brain and serve there for blocking Aβ oligomerization right at the source of the amyloid disease cascade.

AUTHOR CONTRIBUTION

Sabine Rauth, Dominik Hinz, Michael Börger, Markus Uhrig, Manuel Mayhaus, Matthias Riemenschneider and Arne Skerra designed the experiments. Sabine Rauth, Dominik Hinz, Michael Börger, Markus Uhrig, Manuel Mayhaus and Arne Skerra performed experiments and analysed the data. Sabine Rauth, Dominik Hinz, Markus Uhrig, Manuel Mayhaus and Arne Skerra wrote the manuscript.

ACKNOWLEDGEMENTS

We thank Pieris AG, Germany, especially Dr Gabriele Matschiner, for providing the Lcn2 phagemid library and Andrea Allersdorfer for assistance with SPR measurements. We also thank Dr Michael Müller, Technische Universität München, for preparation of the SPOT membrane. PC12 cells were a kind gift from Dr Patricia Rusu, University of Heidelberg, Germany.

CONFLICT OF INTEREST

Arne Skerra is founder and shareholder of Pieris Pharmaceuticals, Inc., the company that commercializes the Anticalin technology for human therapy.

FUNDING

This work was supported by the Bundesministerium für Bildung und Forschung, Germany [grant number 01GU0521 (ARREST-AD) (to A.S. and M.R.)]; and the Schering Foundation, Germany (to S.R.).

REFERENCES

1 Morgan, D. (2011) Immunotherapy for Alzheimer's disease. J. Intern. Med. **269**, 54–63 CrossRef PubMed
2 Tanzi, R.E. and Bertram, L. (2005) Twenty years of the Alzheimer's disease amyloid hypothesis: a genetic perspective. Cell **120**, 545–555 CrossRef PubMed
3 Querfurth, H.W. and LaFerla, F.M. (2010) Alzheimer's disease. N. Engl. J. Med. **362**, 329–344 CrossRef PubMed
4 Kang, J., Lemaire, H.G., Unterbeck, A., Salbaum, J.M., Masters, C.L., Grzeschik, K.H., Multhaup, G., Beyreuther, K. and Müller-Hill, B. (1987) The precursor of Alzheimer's disease amyloid A4 protein resembles a cell-surface receptor. Nature **325**, 733–736 CrossRef PubMed

5 Stine, Jr, W.B., Dahlgren, K.N., Krafft, G.A. and LaDu, M.J. (2003) *In vitro* characterization of conditions for amyloid-β peptide oligomerization and fibrillogenesis. J. Biol. Chem. **278**, 11612–11622 CrossRef PubMed

6 Hardy, J. and Selkoe, D.J. (2002) The amyloid hypothesis of Alzheimer's disease: progress and problems on the road to therapeutics. Science **297**, 353–356 CrossRef PubMed

7 Haass, C. and Selkoe, D.J. (2007) Soluble protein oligomers in neurodegeneration: lessons from the Alzheimer's amyloid β-peptide. Nat. Rev. Mol. Cell. Biol. **8**, 101–112 CrossRef PubMed

8 Walsh, D.M., Klyubin, I., Fadeeva, J.V., Cullen, W.K., Anwyl, R., Wolfe, M.S., Rowan, M.J. and Selkoe, D.J. (2002) Naturally secreted oligomers of amyloid beta protein potently inhibit hippocampal long-term potentiation *in vivo*. Nature **416**, 535–539 CrossRef PubMed

9 McDonald, R.J., Craig, L.A. and Hong, N.S. (2010) The etiology of age-related dementia is more complicated than we think. Behav. Brain Res. **214**, 3–11 CrossRef PubMed

10 Citron, M. (2010) Alzheimer's disease: strategies for disease modification. Nat. Rev. Drug Discov. **9**, 387–398 CrossRef PubMed

11 Doody, R.S., Raman, R., Farlow, M., Iwatsubo, T., Vellas, B., Joffe, S., Kieburtz, K., He, F., Sun, X. and Thomas, R.G. (2013) A phase 3 trial of semagacestat for treatment of Alzheimer's disease. N. Engl. J. Med. **369**, 341–350 CrossRef PubMed

12 Lannfelt, L., Moller, C., Basun, H., Osswald, G., Sehlin, D., Satlin, A., Logovinsky, V. and Gellerfors, P. (2014) Perspectives on future Alzheimer therapies: amyloid-β protofibrils – a new target for immunotherapy with BAN2401 in Alzheimer's disease. Alzheimers Res. Ther. **6**, 16 CrossRef PubMed

13 Delrieu, J., Ousset, P.J., Caillaud, C. and Vellas, B. (2012) 'Clinical trials in Alzheimer's disease': immunotherapy approaches. J. Neurochem. **120** Suppl 1, 186–193 CrossRef PubMed

14 Brody, D.L. and Holtzman, D.M. (2008) Active and passive immunotherapy for neurodegenerative disorders. Annu. Rev. Neurosci. **31**, 175–193 CrossRef PubMed

15 Qian, X., Hamad, B. and Dias-Lalcaca, G. (2015) The Alzheimer disease market. Nat. Rev. Drug Discov. **14**, 675–676 CrossRef PubMed

16 Orgogozo, J.M., Gilman, S., Dartigues, J.F., Laurent, B., Puel, M., Kirby, L.C., Jouanny, P., Dubois, B., Eisner, L. and Flitman, S. (2003) Subacute meningoencephalitis in a subset of patients with AD after Aβ42 immunization. Neurology **61**, 46–54 CrossRef PubMed

17 Robinson, S.R., Bishop, G.M., Lee, H.G. and Munch, G. (2004) Lessons from the AN 1792 Alzheimer vaccine: lest we forget. Neurobiol. Aging **25**, 609–615 CrossRef PubMed

18 DeMattos, R.B., Bales, K.R., Cummins, D.J., Dodart, J.C., Paul, S.M. and Holtzman, D.M. (2001) Peripheral anti-Aβ antibody alters CNS and plasma Aβ clearance and decreases brain Aβ burden in a mouse model of Alzheimer's disease. Proc. Natl. Acad. Sci. U.S.A. **98**, 8850–8855 CrossRef PubMed

19 Bacskai, B.J., Kajdasz, S.T., McLellan, M.E., Games, D., Seubert, P., Schenk, D. and Hyman, B.T. (2002) Non-Fc-mediated mechanisms are involved in clearance of amyloid-β *in vivo* by immunotherapy. J. Neurosci. **22**, 7873–7878 PubMed

20 Medecigo, M., Manoutcharian, K., Vasilevko, V., Govezensky, T., Munguia, M.E., Becerril, B., Luz-Madrigal, A., Vaca, L., Cribbs, D.H. and Gevorkian, G. (2010) Novel amyloid-beta specific scFv and VH antibody fragments from human and mouse phage display antibody libraries. J. Neuroimmunol. **223**, 104–114 CrossRef PubMed

21 Cattepoel, S., Hanenberg, M., Kulic, L. and Nitsch, R.M. (2011) Chronic intranasal treatment with an anti-Aβ_{30-42} scFv antibody ameliorates amyloid pathology in a transgenic mouse model of Alzheimer's disease. PLoS One **6**, e18296 CrossRef PubMed

22 Habicht, G., Haupt, C., Friedrich, R.P., Hortschansky, P., Sachse, C., Meinhardt, J., Wieligmann, K., Gellermann, G.P., Brodhun, M. and Gotz, J. (2007) Directed selection of a conformational antibody domain that prevents mature amyloid fibril formation by stabilizing Aβ protofibrils. Proc. Natl. Acad. Sci. U.S.A. **104**, 19232–19237 CrossRef PubMed

23 Morgado, I., Wieligmann, K., Bereza, M., Ronicke, R., Meinhardt, K., Annamalai, K., Baumann, M., Wacker, J., Hortschansky, P. and Malesevic, M. (2012) Molecular basis of β-amyloid oligomer recognition with a conformational antibody fragment. Proc. Natl. Acad. Sci. U.S.A. **109**, 12503–12508 CrossRef PubMed

24 Grönwall, C., Jonsson, A., Lindström, S., Gunneriusson, E., Ståhl, S. and Herne, N. (2007) Selection and characterization of Affibody ligands binding to Alzheimer amyloid β peptides. J. Biotechnol. **128**, 162–183 CrossRef PubMed

25 Hoyer, W., Grönwall, C., Jonsson, A., Ståhl, S. and Härd, T. (2008) Stabilization of a β-hairpin in monomeric Alzheimer's amyloid-β peptide inhibits amyloid formation. Proc. Natl. Acad. Sci. U.S.A. **105**, 5099–5104 CrossRef PubMed

26 Hanenberg, M., McAfoose, J., Kulic, L., Welt, T., Wirth, F., Parizek, P., Strobel, L., Cattepoel, S., Spani, C. and Derungs, R. (2014) Amyloid-β peptide-specific DARPins as a novel class of potential therapeutics for Alzheimer disease. J. Biol. Chem. **289**, 27080–27089 CrossRef PubMed

27 Richter, A., Eggenstein, E. and Skerra, A. (2014) Anticalins: exploiting a non-Ig scaffold with hypervariable loops for the engineering of binding proteins. FEBS Lett. **588**, 213–218

28 Åkerström, B., Borregaard, N., Flower, D.A. and Salier, J.-S. (2006) Lipocalins., Landes Bioscience, Georgetown, Texas

29 Schiefner, A. and Skerra, A. (2015) The menagerie of human lipocalins: a natural protein scaffold for molecular recognition of physiological compounds. Acc. Chem. Res. **48**, 976–985 CrossRef PubMed

30 Skerra, A. (2000) Lipocalins as a scaffold. Biochim. Biophys. Acta **1482**, 337–350 CrossRef PubMed

31 Gebauer, M. and Skerra, A. (2012) Anticalins: small engineered binding proteins based on the lipocalin scaffold. Methods Enzymol. **503**, 157–188 CrossRef PubMed

32 Kim, H.J., Eichinger, A. and Skerra, A. (2009) High-affinity recognition of lanthanide(III) chelate complexes by a reprogrammed human lipocalin 2. J. Am. Chem. Soc. **131**, 3565–3576 CrossRef PubMed

33 Schönfeld, D., Matschiner, G., Chatwell, L., Trentmann, S., Gille, H., Hülsmeyer, M., Brown, N., Kaye, P.M., Schlehuber, S., Hohlbaum, A.M. and Skerra, A. (2009) An engineered lipocalin specific for CTLA-4 reveals a combining site with structural and conformational features similar to antibodies. Proc. Natl. Acad. Sci. U.S.A. **106**, 8198–8203 CrossRef PubMed

34 Gebauer, M., Schiefner, A., Matschiner, G. and Skerra, A. (2013) Combinatorial design of an Anticalin directed against the extra-domain B for the specific targeting of oncofetal fibronectin. J. Mol. Biol. **425**, 780–802 CrossRef PubMed

35 Goetz, D.H., Holmes, M.A., Borregaard, N., Bluhm, M.E., Raymond, K.N. and Strong, R.K. (2002) The neutrophil lipocalin NGAL is a bacteriostatic agent that interferes with siderophore-mediated iron acquisition. Mol. Cell. **10**, 1033–1043 CrossRef PubMed

36 Zagorski, M.G., Yang, J., Shao, H., Ma, K., Zeng, H. and Hong, A. (1999) Methodological and chemical factors affecting amyloid β peptide amyloidogenicity. Methods Enzymol. **309**, 189–204 CrossRef PubMed

37 Morales, R., Estrada, L.D., Diaz-Espinoza, R., Morales-Scheihing, D., Jara, M.C., Castilla, J. and Soto, C. (2010) Molecular cross talk between misfolded proteins in animal models of Alzheimer's and prion diseases. J. Neurosci. **30**, 4528–4535 CrossRef PubMed

38 Lee, S., Fernandez, E.J. and Good, T.A. (2007) Role of aggregation conditions in structure, stability, and toxicity of intermediates in the Aβ fibril formation pathway. Protein Sci. **16**, 723–732 CrossRef PubMed

39 Hortschansky, P., Schroeckh, V., Christopeit, T., Zandomeneghi, G. and Fändrich, M. (2005) The aggregation kinetics of Alzheimer's β-amyloid peptide is controlled by stochastic nucleation. Protein Sci. **14**, 1753–1759 CrossRef PubMed

40 Skerra, A. (1994) Use of the tetracycline promoter for the tightly regulated production of a murine antibody fragment in *Escherichia coli*. Gene **151**, 131–135 CrossRef PubMed

41 Essen, L.-O. and Skerra, A. (1994) The *de novo* design of an antibody combining site. Crystallographic analysis of the V_L domain confirms the structural model. J. Mol. Biol. **238**, 226–244 CrossRef PubMed

42 Yanisch-Perron, C., Vieira, J. and Messing, J. (1985) Improved M13 phage cloning vectors and host strains: nucleotide sequences of the M13mp18 and pUC19 vectors. Gene **33**, 103–119 CrossRef PubMed

43 Moretto, N., Bolchi, A., Rivetti, C., Imbimbo, B.P., Villetti, G., Pietrini, V., Polonelli, L., Del Signore, S., Smith, K.M., Ferrante, R.J. and Ottonello, S. (2007) Conformation-sensitive antibodies against Alzheimer amyloid-β by immunization with a thioredoxin-constrained B-cell epitope peptide. J. Biol. Chem. **282**, 11436–11445 CrossRef PubMed

44 Fling, S.P. and Gregerson, D.S. (1986) Peptide and protein molecular weight determination by electrophoresis using a high-molarity tris buffer system without urea. Anal. Biochem. **155**, 83–88 CrossRef PubMed

45 Gasteiger, E., Gattiker, A., Hoogland, C., Ivanyi, I., Appel, R.D. and Bairoch, A. (2003) ExPASy: the proteomics server for in-depth protein knowledge and analysis. Nucleic Acids Res. **31**, 3784–3788 CrossRef PubMed

46 Breustedt, D.A., Schönfeld, D.L. and Skerra, A. (2006) Comparative ligand-binding analysis of ten human lipocalins. Biochim. Biophys. Acta **1764**, 161–173 CrossRef PubMed

47 Skerra, A., Gebauer, M., Hinz, D., Rauth, S. and Matschiner, G. (2011) Muteins of human lipocalin 2 (Lcn2, hNGAL) with affinity for a given target. WO 2011/069992 A2

48 Bullock, W.O., Fernandez, J.M. and Short, J.M. (1987) XL1-Blue: a high efficiency plasmid transforming *rec*A *Escherichia coli* strain with β-galactosidase selection. BioTechniques **5**, 376–379

49 Schmidt, T.G. and Skerra, A. (2007) The *Strep*-tag system for one-step purification and high-affinity detection or capturing of proteins. Nat. Protoc. **2**, 1528–1535 CrossRef PubMed

50 Jensen, K.F. (1993) The *Escherichia coli* K-12 "wild types" W3110 and MG1655 have an *rph* frameshift mutation that leads to pyrimidine starvation due to low *pyrE* expression levels. J. Bacteriol. **175**, 3401–3407 PubMed

51 Studier, F.W. and Moffatt, B.A. (1986) Use of bacteriophage T7 RNA polymerase to direct selective high-level expression of cloned genes. J. Mol. Biol. **189**, 113–130 CrossRef PubMed

52 Schlehuber, S. and Skerra, A. (2002) Tuning ligand affinity, specificity, and folding stability of an engineered lipocalin variant – a so-called 'anticalin' – using a molecular random approach. Biophys. Chem. **96**, 213–228 CrossRef PubMed

53 Myszka, D.G. (1999) Improving biosensor analysis. J. Mol. Recognit. **12**, 279–284 CrossRef PubMed

54 Karlsson, R., Michaelsson, A. and Mattsson, L. (1991) Kinetic analysis of monoclonal antibody-antigen interactions with a new biosensor based analytical system. J. Immunol. Methods **145**, 229–240 CrossRef PubMed

55 Frank, R. (2002) The SPOT-synthesis technique. Synthetic peptide arrays on membrane supports – principles and applications. J. Immunol. Methods **267**, 13–26 CrossRef PubMed

56 Zander, H., Reineke, U., Schneider-Mergener, J. and Skerra, A. (2007) Epitope mapping of the neuronal growth inhibitor Nogo-A for the Nogo receptor and the cognate monoclonal antibody IN-1 by means of the SPOT technique. J. Mol. Recognit. **20**, 185–196 CrossRef PubMed

57 Sabaté, R., Gallardo, M. and Estelrich, J. (2003) An autocatalytic reaction as a model for the kinetics of the aggregation of β-amyloid. Biopolymers **71**, 190–195 CrossRef PubMed

58 Finder, V.H. and Glockshuber, R. (2007) Amyloid-β aggregation. Neurodegener. Dis. **4**, 13–27 CrossRef PubMed

59 Schlehuber, S., Beste, G. and Skerra, A. (2000) A novel type of receptor protein, based on the lipocalin scaffold, with specificity for digoxigenin. J. Mol. Biol. **297**, 1105–1120 CrossRef PubMed

60 LeVine, 3rd, H. (1999) Quantification of β-sheet amyloid fibril structures with thioflavin T. Methods Enzymol. **309**, 274–284 CrossRef PubMed

61 Jarrett, J.T. and Lansbury, Jr, P.T. (1993) Seeding "one-dimensional crystallization" of amyloid: a pathogenic mechanism in Alzheimer's disease and scrapie? Cell **73**, 1055–1058 CrossRef PubMed

62 Manzoni, C., Colombo, L., Messa, M., Cagnotto, A., Cantu, L., Del Favero, E. and Salmona, M. (2009) Overcoming synthetic Aβ peptide aging: a new approach to an age-old problem. Amyloid **16**, 71–80 CrossRef PubMed

63 Jan, A., Hartley, D.M. and Lashuel, H.A. (2010) Preparation and characterization of toxic Aβ aggregates for structural and functional studies in Alzheimer's disease research. Nat. Protoc. **5**, 1186–1209 CrossRef PubMed

64 Ramakrishnan, M., Kandimalla, K.K., Wengenack, T.M., Howell, K.G. and Poduslo, J.F. (2009) Surface plasmon resonance binding kinetics of Alzheimer's disease amyloid β peptide-capturing and plaque-binding monoclonal antibodies. Biochemistry **48**, 10405–10415 CrossRef PubMed

65 Moreira, P., Pereira, C., Santos, M.S. and Oliveira, C. (2000) Effect of zinc ions on the cytotoxicity induced by the amyloid β-peptide. Antioxid. Redox Signal. **2**, 317–325 CrossRef PubMed

66 Varadarajan, S., Yatin, S., Aksenova, M. and Butterfield, D.A. (2000) Review: Alzheimer's amyloid β-peptide-associated free radical oxidative stress and neurotoxicity. J. Struct. Biol. **130**, 184–208 CrossRef PubMed

67 Sun, X., Chen, W.D. and Wang, Y.D. (2015) β-Amyloid: the key peptide in the pathogenesis of Alzheimer's disease. Front. Pharmacol. **6**, 221 PubMed

68 Pivtoraiko, V.N., Abrahamson, E.E., Leurgans, S.E., DeKosky, S.T., Mufson, E.J. and Ikonomovic, M.D. (2015) Cortical pyroglutamate amyloid-β levels and cognitive decline in Alzheimer's disease. Neurobiol. Aging **36**, 12–19 CrossRef PubMed

69 Haupt, C. and Fändrich, M. (2014) Biotechnologically engineered protein binders for applications in amyloid diseases. Trends Biotechnol. **32**, 513–520 CrossRef PubMed

70 Luheshi, L.M., Hoyer, W., de Barros, T.P., van Dijk Härd, I., Brorsson, A.C., Macao, B., Persson, C., Crowther, D.C., Lomas, D.A. and Ståhl, S. (2010) Sequestration of the Aβ peptide prevents toxicity and promotes degradation in vivo. PLoS Biol. **8**, e1000334 CrossRef PubMed

71 Wacker, J., Rönicke, R., Westermann, M., Wulff, M., Reymann, K.G., Dobson, C.M., Horn, U., Crowther, D.C., Luheshi, L.M. and Fändrich, M. (2014) Oligomer-targeting with a conformational antibody fragment promotes toxicity in Aβ-expressing flies. Acta Neuropathol. Commun. **2**, 43 CrossRef PubMed

72 Tjernberg, L.O., Naslund, J., Lindqvist, F., Johansson, J., Karlstrom, A.R., Thyberg, J., Terenius, L. and Nordstedt, C. (1996) Arrest of β-amyloid fibril formation by a pentapeptide ligand. J. Biol. Chem. **271**, 8545–8548 CrossRef PubMed

73 Abelein, A., Abrahams, J.P., Danielsson, J., Gräslund, A., Jarvet, J., Luo, J., Tiiman, A. and Wärmländer, S.K. (2014) The hairpin conformation of the amyloid β peptide is an important structural motif along the aggregation pathway. J. Biol. Inorg. Chem. **19**, 623–634 CrossRef PubMed

74 Lichtenthaler, S.F. (2011) α-secretase in Alzheimer's disease: molecular identity, regulation and therapeutic potential. J. Neurochem. **116**, 10–21 CrossRef PubMed

75 Bateman, R.J., Aisen, P.S., De Strooper, B., Fox, N.C., Lemere, C.A., Ringman, J.M., Salloway, S., Sperling, R.A., Windisch, M. and Xiong, C. (2011) Autosomal-dominant Alzheimer's disease: a review and proposal for the prevention of Alzheimer's disease. Alzheimers Res. Ther. **3**, 1 CrossRef PubMed

76 Nilsberth, C., Westlind-Danielsson, A., Eckman, C.B., Condron, M.M., Axelman, K., Forsell, C., Stenh, C., Luthman, J., Teplow, D.B. and Younkin, S.G. (2001) The 'Arctic' APP mutation (E693G) causes Alzheimer's disease by enhanced Aβ protofibril formation. Nat. Neurosci. **4**, 887–893 CrossRef PubMed

77 Levy, E., Carman, M.D., Fernandez-Madrid, I.J., Power, M.D., Lieberburg, I., van Duinen, S.G., Bots, G.T., Luyendijk, W. and Frangione, B. (1990) Mutation of the Alzheimer's disease amyloid gene in hereditary cerebral hemorrhage, Dutch type. Science **248**, 1124–1126 CrossRef PubMed

78 Tagliavini, F., Rossi, G., Padovani, A., Magoni, M., Andora, G., Sgarzi, M., Bizzi, A., Savoiardo, M., Carella, F. and Morbin, M. (1999) A new βPP mutation related to hereditary cerebral haemorrhage. Alzheimer's Rep. **2**, S28

79 Grabowski, T.J., Cho, H.S., Vonsattel, J.P., Rebeck, G.W. and Greenberg, S.M. (2001) Novel amyloid precursor protein mutation in an Iowa family with dementia and severe cerebral amyloid angiopathy. Ann. Neurol. **49**, 697–705 CrossRef PubMed

80 Tycko, R., Sciarretta, K.L., Orgel, J.P. and Meredith, S.C. (2009) Evidence for novel β-sheet structures in Iowa mutant β-amyloid fibrils. Biochemistry **48**, 6072–6084 CrossRef PubMed

81 Hendriks, L., van Duijn, C.M., Cras, P., Cruts, M., Van Hul, W., van Harskamp, F., Warren, A., McInnis, M.G., Antonarakis, S.E., Martin, J.J. et al. (1992) Presenile dementia and cerebral haemorrhage linked to a mutation at codon 692 of the β-amyloid precursor protein gene. Nat. Genet. **1**, 218–221 CrossRef PubMed

82 Lührs, T., Ritter, C., Adrian, M., Riek-Loher, D., Bohrmann, B., Dobeli, H., Schubert, D. and Riek, R. (2005) 3D structure of Alzheimer's amyloid-β(1–42) fibrils. Proc. Natl. Acad. Sci. U.S.A. **102**, 17342–17347 CrossRef PubMed

83 Makin, O.S., Atkins, E., Sikorski, P., Johansson, J. and Serpell, L.C. (2005) Molecular basis for amyloid fibril formation and stability. Proc. Natl. Acad. Sci. U.S.A. **102**, 315–320 CrossRef PubMed

84 Austen, B.M., Paleologou, K.E., Ali, S.A., Qureshi, M.M., Allsop, D. and El-Agnaf, O.M. (2008) Designing peptide inhibitors for oligomerization and toxicity of Alzheimer's β-amyloid peptide. Biochemistry **47**, 1984–1992 CrossRef PubMed

85 Soto, C., Sigurdsson, E.M., Morelli, L., Kumar, R.A., Castano, E.M. and Frangione, B. (1998) β-sheet breaker peptides inhibit fibrillogenesis in a rat brain model of amyloidosis: implications for Alzheimer's therapy. Nat. Med. **4**, 822–826 CrossRef PubMed

86 Legleiter, J., Czilli, D.L., Gitter, B., DeMattos, R.B., Holtzman, D.M. and Kowalewski, T. (2004) Effect of different anti-Aβ antibodies on Abeta fibrillogenesis as assessed by atomic force microscopy. J. Mol. Biol. **335**, 997–1006 CrossRef PubMed

87 Lichtlen, P. and Mohajeri, M.H. (2008) Antibody-based approaches in Alzheimer's research: safety, pharmacokinetics, metabolism, and analytical tools. J. Neurochem. **104**, 859–874 CrossRef PubMed

88 Salloway, S., Sperling, R., Fox, N.C., Blennow, K., Klunk, W., Raskind, M., Sabbagh, M., Honig, L.S., Porsteinsson, A.P. and Ferris, S. (2014) Two phase 3 trials of bapineuzumab in mild-to-moderate Alzheimer's disease. N. Engl. J. Med. **370**, 322–333 CrossRef PubMed

89 Doody, R.S., Thomas, R.G., Farlow, M., Iwatsubo, T., Vellas, B., Joffe, S., Kieburtz, K., Raman, R., Sun, X. and Aisen, P.S. (2014) Phase 3 trials of solanezumab for mild-to-moderate Alzheimer's disease. N. Engl. J. Med. **370**, 311–321 CrossRef PubMed

90 Siemers, E.R., Friedrich, S., Dean, R.A., Gonzales, C.R., Farlow, M.R., Paul, S.M. and Demattos, R.B. (2010) Safety and changes in plasma and cerebrospinal fluid amyloid β after a single administration of an amyloid β monoclonal antibody in subjects with Alzheimer disease. Clin. Neuropharmacol. **33**, 67–73 CrossRef PubMed

91 Karran, E. and Hardy, J. (2014) Antiamyloid therapy for Alzheimer's disease – are we on the right road? N. Engl. J. Med. **370**, 377–378 CrossRef PubMed

92 Villemagne, V.L., Burnham, S., Bourgeat, P., Brown, B., Ellis, K.A., Salvado, O., Szoeke, C., Macaulay, S.L., Martins, R. and Maruff, P. (2013) Amyloid β deposition, neurodegeneration, and cognitive decline in sporadic Alzheimer's disease: a prospective cohort study. Lancet Neurol. **12**, 357–367 CrossRef PubMed

93 Bateman, R.J., Xiong, C., Benzinger, T.L., Fagan, A.M., Goate, A., Fox, N.C., Marcus, D.S., Cairns, N.J., Xie, X. and Blazey, T.M. (2012) Clinical and biomarker changes in dominantly inherited Alzheimer's disease. N. Engl. J. Med. **367**, 795–804 CrossRef PubMed

94 Panza, F., Solfrizzi, V., Imbimbo, B.P., Tortelli, R., Santamato, A. and Logroscino, G. (2014) Amyloid-based immunotherapy for Alzheimer's disease in the time of prevention trials: the way forward. Expert Rev. Clin. Immunol. **10**, 405–419 CrossRef PubMed

95 Crespi, G.A., Hermans, S.J., Parker, M.W. and Miles, L.A. (2015) Molecular basis for mid-region amyloid-β capture by leading Alzheimer's disease immunotherapies. Sci. Rep. **5**, 9649 CrossRef PubMed

96 DeMattos, R.B., Bales, K.R., Cummins, D.J., Paul, S.M. and Holtzman, D.M. (2002) Brain to plasma amyloid-β efflux: a measure of brain amyloid burden in a mouse model of Alzheimer's disease. Science **295**, 2264–2267 CrossRef PubMed

97 Farlow, M., Arnold, S.E., van Dyck, C.H., Aisen, P.S., Snider, B.J., Porsteinsson, A.P., Friedrich, S., Dean, R.A., Gonzales, C. and Sethuraman, G. (2012) Safety and biomarker effects of solanezumab in patients with Alzheimer's disease. Alzheimers Dement. **8**, 261–271 CrossRef PubMed

98 Sperling, R.A., Jack, Jr, C.R., Black, S.E., Frosch, M.P., Greenberg, S.M., Hyman, B.T., Scheltens, P., Carrillo, M.C., Thies, W. and Bednar, M.M. (2011) Amyloid-related imaging abnormalities in amyloid-modifying therapeutic trials: recommendations from the Alzheimer's Association Research Roundtable Workgroup. Alzheimers Dement. **7**, 367–385 CrossRef PubMed

99 Boado, R.J., Lu, J.Z., Hui, E.K. and Pardridge, W.M. (2010) IgG-single chain Fv fusion protein therapeutic for Alzheimer's disease: expression in CHO cells and pharmacokinetics and brain delivery in the rhesus monkey. Biotechnol. Bioeng. **105**, 627–635 CrossRef PubMed

100 Niewoehner, J., Bohrmann, B., Collin, L., Urich, E., Sade, H., Maier, P., Rueger, P., Stracke, J.O., Lau, W., Tissot, A.C. et al. (2014) Increased brain penetration and potency of a therapeutic antibody using a monovalent molecular shuttle. Neuron **81**, 49–60 CrossRef PubMed

Received 14 February 2016/26 March 2016; accepted 30 March 2016
Accepted Manuscript online 30 March 2016, doi:10.1042/BCJ20160114